AN INTEGRATED COMPUTATIONAL & EXPERIMENTAL STUDY OF STIFFNESS BEHAVIOR OF 6-DOF PLATFORM TOP PLATE SUBJECTED TO VARIOUS JOINT & LOADING CONDITIONS

Author
UMAR NAWAZ BHATTI
MS-68 (Mechanical Engineering)
(2011-NUST-MS PhD- Mech-27)

THESIS

Submitted to the Department of Mechanical Engineering in Fulfillment of the Requirements for the Degree of

MASTER OF SCIENCE

in

MECHANICAL ENGINEERING

Thesis Supervisor

Dr. Aamer A. Baqai

College of Electrical & Mechanical Engineering
National University of Sciences & Technology
January, 2015

Copyright Statement

AN INTEGRATED COMPUTATIONAL & EXPERIMENTAL STUDY OF STIFFNESS BEHAVIOR OF 6-DOF PLATFORM TOP PLATE SUBJECTED TO VARIOUS JOINT & LOADING CONDITIONS

By

Umar Nawaz Bhatti

Submitted to the Faculty of Department of Mechanical Engineering, National University of Sciences and Technology College of Electrical and Mechanical Engineering, Rawalpindi Pakistan, in partial fulfillment of the requirement for the degree of Master of Science in Mechanical Engineering

Candidate: _____

Umar Nawaz Bhatti

Advisor: _____

Dr. Aamer A. Baqai

Guidance and Evaluation Committee (GEC) Members:

1. Assistant Prof. Dr. Hasan Aftab Saeed
2. Assistant Prof. Dr. Sajid Ullah Butt
3. Dr. Wasim Akram

National University of Sciences and Technology,
College of Electrical & Mechanical Engineering,
Rawalpindi.

26th December, 2014

ABSTRACT

Research and development of various parallel mechanism/manipulator applications in engineering are now being performed more and more actively in every industrial field. Simulation driven designs are used for the efficient development of these high precision devices. Accurate prediction of these simulations depend upon the fact that how closely actual conditions are incorporated in the analysis.

Stiffness is a key property for parallel platforms as it is directly affects the positional accuracy of system. It is directly related to deformations in mechanisms. These deformations in parallel platforms have adverse effects on static and fatigue strength, reduces wear resistance & efficiency in terms of frictional losses. Thus compromising the dynamic stability and accuracy of the system. Modeling the static and dynamic stiffness is the lead up for optimizing the mechanical structure, which in turns aides in development of efficient control system.

Overall stiffness of the platforms is not only driven by the stiffness of the links but also by contact stiffness of joints. For large heavily loaded manipulators, top plate presents itself as critical component; as it shares a major percentage of the cumulative mechanism's weight. Consequently, top plate stiffness will dominate the overall stiffness of platform throughout the regular workspace. This makes the operational accuracy and safe working of the system largely dependent on accurate modeling of top plate's stiffness.

In this thesis, an accurate stiffness modeling methodology is proposed for special application of 6-DOF platforms i.e. subjected to heavy loads. Effect of joint contact conditions on both static and dynamic stiffness behavior of platform's top plate is analyzed. Top plate was designed using simplified loading and joint contact conditions. A prototype was developed using this design and failed when tested on operating conditions. Detailed design was carried out using actual loading conditions and introducing the realistic joint contact formulation. Resulting stiffness parameters obtained were found to be in good agreement with experimental results.

The findings of this work are used as an additional index to find an optimum compromise between a lightweight design and the stiffness performance of top plate by performing multi-objective structural optimization. Design of the top plate was optimized for size and shape in order to minimize the mass in motion while guaranteeing a desired stiffness through-out a

regular workspace of the mechanism. Stiffness behavior of optimized structure matched the experimental results when developed and tested.

To my beloved parents and family….

ACKNOWLEDGEMENT

First and foremost, I would like to thank my Almighty Allah for all His blessings and benevolence which helped me complete this incredible task in terms of integrity and completeness.

Secondly, there is long list of people without whom I would not have been to complete this endeavor successfully. I would like to communicate my special appreciation and gratitude to my advisor, Dr. Aamer Ahmed Baqai for his extended support throughout my thesis tenure. His untiring efforts and advice helped me move around the tight corners during my research work. His constant support helped me to be consistent and productive, for which he has my utter gratitude.

I would also like to pay special thanks to my co advisor Dr. Wasim Akram whose guidance served as beacon of light and inspiration throughout my research work. His professional experience proved invaluable for completing the experimental and testing phase for this project.

I would also like to thank Assistant Professor Dr. Sajid Ullah Butt and Assistant Professor Dr. Hasan Aftab Saeed, for serving as my Guidance and Evaluation committee even at hardship. I am really obliged for letting my defense be an enjoyable moment, and for their brilliant comments and suggestions.

A special thanks to my family; my mother, father and siblings, for all the sacrifices that they have made on my behalf and who were always in my support in dire moments.

Conclusively, I would like to thank the entire honorable faculty of Department of Mechanical Engineering, whose professional approach and vision groomed me as a sound person both technically and morally.

Umar Nawaz Bhatti

December, 2014

TABLE OF CONTENTS Page No.

ABSTRACT iv

ACKNOWLEDGEMENT vii

LIST OF TABLES xi

LIST OF FIGURES xiii

LIST OF ABBREVIATIONS xvi

CHAPTER 1

INTRODUCTION 1

CHAPTER 2 5

LITERATURE REVIEW 5

1. Parallel Manipulators 5
2. Stiffness analysis of parallel manipulators 6
   - i. Matrix Structure Analysis (MSA) 7
   - ii. Virtual Joint Method (VJM) 8
   - iii. Finite Element Analysis (FEA) 9
3. Joints & mechanical stiffness of manipulators 11
4. Optimization 12
5. Motivation 13
6. Objectives 14

CHAPTER 3

MODELING AND METHODOLOGY 15

1. Top plate design 15
2. Simplified modeling 18
   - i. Parametric Modeling of Initial Design 18
   - ii. Simplified FEM Modeling 18
   - iii. Prototype Development and Physical Experiments 19
   - iv. Evaluation of Simplified Results 19
3. Detailed Modeling 19
   - i. Detailed FEM Modeling 19
   - ii. Physical Experiments 20

4. Top plate optimization 20
i. Size Optimization 21
ii. Shape Optimization 21
iii. Prototype Development and Physical Experiments 22
iv. Evaluation of Optimized Results 23

CHAPTER 4
BOUNDARY CONDITIONS EFFECT ANALYSIS 24
1. Top plate design 24
2. Simplified modeling 26
i. FEM Results 26
ii. Experimental Setup 28
iii. Results Correlation and Evaluation 29
3. Detailed Modeling 29
i. Area Contact Analysis Results 29
ii. Line Contact Analysis Results 30
iii. Results Correlation and Evaluation 32

CHAPTER 5
TOP PLATE OPTIMIZATION 34
1. Size optimization 34
i. DOE Matrix 35
ii. Response Surface 35
iii. Sensitivity Analysis 38
iv. Optimization 39
2. Shape optimization 44
Case 1 45
i. DOE Matrix 45
ii. Response Surface 46
iii. Sensitivity Analysis 50
iv. Optimization 50
Case 2 51
i. DOE Matrix 51

ii. Response Surface 52
iii. Optimization 53
4. FEM Results 54
5. Experimental testing 56
6. Evaluation of results 56
FUTURE SCOPE **58**
CONCLUSION **59**
REFERENCES **61**

LIST OF TABLES

Page No.

Table 1. Broad requirements for top plate design 15

Table 2. Task load specifications 20

Table 3. Material properties of Structural Steel 25

Table 4. Stiffness response of initial design of top plate 25

Table 5. Specification of initial design of top plate 25

Table 6. Static stiffness results for simplified FEM model 27

Table 7. Dynamic stiffness results for simplified FEM model 27

Table 8. Experimental values for top plate designed (pre-optimized) 29

Table 9. Relative error between experimental & simplified FEA results 29

Table 10. Static stiffness results for detailed FEM modeling 30

Table 11. Dynamic stiffness results for detailed FEM modeling 30

Table 12. Relative error between experimental & detailed FEA results 32

Table 13. Optimum candidate points obtained using screening optimization [Max freq] 41

Table 14. Optimum candidate points obtained using MOGA optimization [Max freq] 41

Table 15. Optimum candidate points obtained using screening [Frequency as goal] 43

Table 16. Optimum candidate points obtained using MOGA [Frequency as goal] 43

Table 17. Optimum candidate points obtained using screening [value greater than 9.5Hz] 43

Table 18. Optimum candidate points obtained using MOGA [value greater than 9.5Hz] 43

Table 19. Salient features of optimum top plate design obtained after size optimization 44

Table 20. Optimum candidate points for shape optimization using MOGA [Case 1] 51

Table 21. Optimum candidate points for shape optimization using MOGA [Case 2] 53

Table 22. Weight Reduction achieved through shape optimization 53

Table 23. Specifications of final optimized design 54

Table 24. FEM results for Static stiffness of optimized design 54

Table 25. FEM results for dynamic stiffness of optimized design 55

Table 26. Experimental values for top plate (Optimized design) 56

Table 27. Relative error between experimental & FEA results (Optimized design) 57

LIST OF FIGURES

Page No.

Figure 1. Two possible cases of vibration isolation 2

Figure 2. 6-DOF (Stewart-Gough) parallel manipulator 5

Figure 3. Methodology flow chart 16

Figure 4. Top plate shape and rib structure used 17

Figure 5. Geometry used for simulating joint attachment. 17

Figure 6. Load applied to simulate payload 18

Figure 7. Height and width parameters used for controlling top plate assembly 21

Figure 8. Height and width parameters used for controlling Top plate assembly 22

Figure 9. Static total deformation for initial design of top plate 26

Figure 10. 1st Mode shape contours initial design for top plate 26

Figure 11. Static total deformation contours (simplified FEM) 27

Figure 12. Mode shape for 1st mode frequency (simplified FEM) 27

Figure 13. Mode shape for 2nd mode frequency (simplified FEM) 28

Figure 14. Mode shape for 3rd mode frequency (simplified FEM) 28

Figure 15. Static total deformation contours (detailed FEM) 30

Figure 16. Mode shape for 1st mode frequency (detailed FEM) 31

Figure 17. Mode shape for 2nd mode frequency (detailed FEM) 31

Figure 18. Mode shape for 3rd mode frequency (detailed FEM) 31

Figure 19. Static deformation variation with joint contact 33

Figure 20. 1st mode frequency variation with joint contact 33

Figure 21. Top plate structure used for size optimization 34

Figure 22. DOE matrix used and results obtained for objectives 35

Figure 23. 1st mode frequency response against design parameters 36

Figure 24. Static deformation response against design parameters 36

Figure 25. Top plate mass response against design parameters 36

Figure 26. 1st mode Frequency (Hz) response 37

Figure 27. Static total deformation (mm) variation 37

Figure 28. Top plate mass (ton) response 37

Figure 29. Local Sensitivity of output parameters with variation in input parameters 38

Figure 30. Sensitivity Curves 39

Figure 31. 3D Trade off charts for maximize frequency (Hz) objective 40

Figure 32. 1st mode frequency (Hz) vs. deformation (mm) [maximize freq] 40

Figure 33. 1st mode frequency (Hz) vs. top plate mass (ton) [maximize freq] 40

Figure 34. 3D Trade off charts for frequency value greater than 9.5Hz objective 42

Figure 35. 1st mode frequency (Hz) vs. static deformation (mm) [value greater than 9.5Hz] 42

Figure 36. 1st mode frequency (Hz) vs. top plate mass (ton) [value greater than 9.5Hz] 42

Figure 37. Preview of top plate design used for shape optimization 44

Figure 38. DOE matrix used for shape optimization [Case 1] 45

Figure 39. 3D response surfaces against DS_outside_height & DS_width parameters 46

Figure 40. 3D response surfaces against DS_total_height & DS_width parameters 47

Figure 41. 3D response surfaces against DS_outside_height & DS_total_height parameters 48

Figure 42. 1st mode Frequency (Hz) variation 48

Figure 43. Static total deformation (mm) variation 49

Figure 44. Top plate mass (ton) variation 50

Figure 45. Local sensitivity of output parameters [Shape optimization Case 1] 50

Figure 46. DOE matrix used for shape optimization [Case 2] 52

Figure 47. Response curves for shape optimization study [Case 2] 52

Figure 48. Static deformation contours (Optimized design) 54

Figure 49. 1st mode shape contours (Optimized design) 55

Figure 50. 2nd mode shape contours (Optimized design) 55

Figure 51. 3rd mode shape contours (Optimized design) 56

LIST OF ABBREVIATIONS

BC	Boundary Conditions
DOF	Degrees of Freedom
DOE	Design of Experiments
FEA	Finite Element Analysis
FEM	Finite Element Methods
FOS	Factor of Safety
GA	Genetic Algorithm
MOGA	Multi objective Genetic Algorithm
MSA	Matrix Structure Analysis
PKM	Parallel Kinematic Manipulator
VJM	Virtual Joint Method

CHAPTER 1

INTRODUCTION

Parallel kinematic manipulators (PKM) have emerged as leading candidate for research during the past few decades. Researchers and manufacturers worldwide are constantly striving for better, safer and cost effective designs (Bonev, 1998). This trend implicates their distinct advantages over serial kinematic manipulators as these manipulators have various serial kinematic chains working in tandem. These advantages are the reason behind their diverse practical application such as motion simulators (Stewart D., 1965), assembly cells (McCallion et. al., 1979), micro-positioning systems, coordinate measuring machines, milling machines, surgery robots (Grace, 1995; Lazarevic, 1997) and many others.

The availability of various serial kinematic chains in PKMs gives them an edge in operational aspects such as higher loading capacity, increased stiffness, and motion redundancy. Consequently, these manipulators prevent buildup of individual errors in various actuators of mechanism (Anderson et al., 2004; Hall et al.,2003). Thus considered as an ideal candidate for applications demanding precise positioning (Memet, 2006).

However, many of manipulator applications are situated in environments where it is hard to completely isolate the system from certain degrees of disturbances. The vibrations resulting from these disturbances have an adverse effect on the performance of the sensitive instruments which are critical for precision positioning. This underlines the need to generate an environment free of such vibrations in order to meet the objective of precise positioning. But designing a whole system free of vibrations is a daunting task as the cost effectiveness and feasibility is very low. Therefore, the disturbances need to be eliminated at the interfaces between either the vibration source and the main structure or the main structure and the sensitive equipment used for precision applications (Figure 1). From a design perspective; 6-DOF manipulator becomes the foremost logical choice for providing such vibration isolation (Memet, 2006).

6-DOF mechanisms have been used in machining processes, simulators, simulation of wave induced motion on naval cargo ships, military applications i.e. to provide a stable platform against ship movement for mounting the turret and space applications. Space applications are the

most promising area of research involving the use of these mechanisms for vibration isolation, where the vibration isolation of precision position equipment is highly critical. (Memet, 2006).

Figure 1. Two possible cases of vibration isolation

The essential performance measuring criteria for most parallel manipulators can be underlined in terms of positioning accuracy and high payload capability, both of which are directly governed by their overall stiffness. Stiffness is defined as mechanical system's capacity to withstand loads without excessive deformation (Aftab, 2012). Failure to keep these deformations within acceptable range can have adverse effects on static/fatigue strength & efficiency in terms of frictional losses; reduces wear resistance, compromises dynamic stability (vibration effects) and accuracy.

Current design trends (mechanical design) of robotic manipulators lay primary emphasis on minimizing the moving masses. This will lead to use of small actuators with improved dynamic performances, thus resulting in an energy efficient design. This instigates the use of advanced kinematical architectures, materials with high strength to weight ratios and cross-sectional area reduction of every critical element. Any such minimization is directly linked to the mechanical stiffness of the manipulator if the desired accuracy and performance is to be achieved (Aftab, 2012).

In general practice, the stiffness is evaluated numerically through the calculation of "stiffness matrix", K. This matrix express the relation between the displacement (translational/rotational) and the forces/torques (Aftab, 2012).

Several different approaches exist for calculation of stiffness matrix. Broad categories are the virtual joint method (VJM), the finite element analysis (FEA) and the matrix structural analysis (MSA). Every one of these approach uses different computational technique and are based on different modeling assumptions. The FEA method has proven to be the most accurate and reliable, because of its ability to model the links/joints exactly to its dimension and shape.

In order to have accurate stiffness models and better match between theoretical and experimental results, special consideration has to be given to joints used in manipulators. Joints play an vital role in mechanical stiffness of parallel manipulators. For parallel manipulators, the most commonly used joints, in increasing order of degrees of freedom are: revolute, prismatic, universal and spherical joints. In most of research, joints are considered as rigid with constant stiffness value. To achieve more realistic results complex effects such as joint stiffness must be incorporated in the stiffness analysis of parallel manipulators as they also play a part in degrading the positioning accuracy.

Having discussed briefly the different aspects and relative factors associated with design of parallel manipulators, it is evident from literature that 6-DOF manipulators are most complex mechanism among the family. Many of its applications, i.e. military, simulators & space launch, involve large platforms with a heavy payload. For such manipulators, top plate presents itself as critical component; as it shares a major percentage of the cumulative mechanism's weight.

Prediction of overall stiffness of a mechanism plays a pivotal role during its design phase. For large and heavily platform applications, top plate stiffness will dominate the overall stiffness of platform throughout the regular workspace. This makes the operational accuracy and safe working of the system largely dependent on accurate modeling of top plate's stiffness.

Conclusively, the thesis to follow has hence, attempted to draft a FEA based simulation methodology where in an algorithmic approach was proposed for accurate prediction of stiffness of 6-DOF platform's top plate. Top plate was subjected to various joint contact conditions and stiffness behavior was analyzed for each of these conditions. Experimental testing was performed on prototype developed based on design for each joint condition. The aim was to achieve a design that presents a perfect match between the simulation and experimental results.

Lastly, an optimization study was performed to obtain a weight optimum design incorporating the actual boundary conditions and ensuring safe working for given operating conditions.

The rest of thesis is organized as follows: **Chapter 2** presents the literature review of some work done on static/dynamic stiffness analysis, joint contact and clearances effect on stiffness, as well as optimization work carried for parallel platform manipulators with special emphasis on 6-DOF manipulators. In **Chapter 3** the methodology adopted for carrying out the work is presented and all the mathematical & technological tools used in this thesis are explored. In **Chapter 4,** the results regarding the effect of different boundary conditions on the stiffness behavior of top plate are discussed. In **Chapter 5,** the results of the optimization study carried out for design of top plate are discussed. Finally, the future scope and conclusions are presented.

CHAPTER 2

LITERATURE REVIEW

1. Parallel Manipulators

General composition of parallel mechanism consists of two platforms connected together by parallel acting legs/joints. The widely used configuration consist of six legs either operated hydraulically (linear actuators) or spring loaded (for passive mechanism). Among the two platforms, upper one is defined as "movable platform or top-plate" and exhibits six degrees of freedom with respect to other one which is fixed and is known as "base". Due to six degrees of freedom, top plate is capable of translating/rotating in all three linear and angular directions either independently or in combination of both, (Dan Zhang, 2000). Gough (1956) was the first to introduce such platform, to be used as tire testing machine, later on Stewart (1965) used the same as an aircraft simulator. The platform is now known as "Gough-Stewart" platform and is continually been investigated by many researchers up-till now (Liu et. al.,2000; Mahmoodi et. al., 2009; Vakil et. al. 2008).

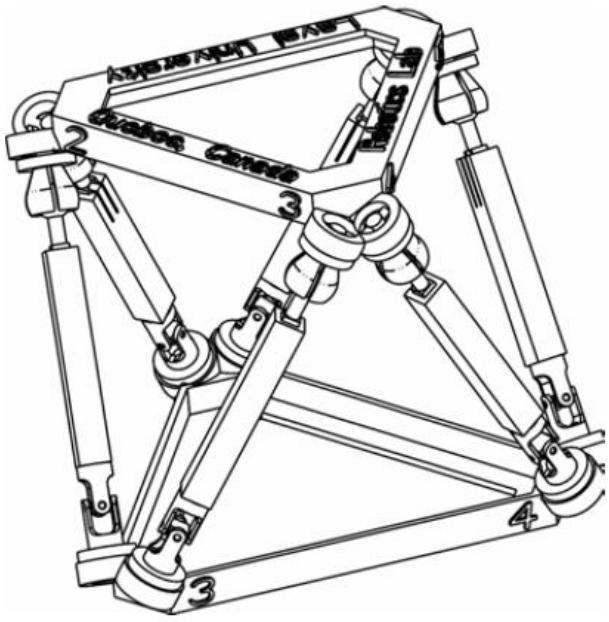

Figure 2. 6-DOF (Stewart-Gough) parallel manipulator

Over the past few years, researchers (e.g., Kohli, Hunt, Bailey etc) and industries have developed a considerable interest in PKMs. This inclination has led to continuous development and refinement of all related research fields. This trend is depicted by many instances that can be seen in recent literature: work is done concerning forward pose solution generation of analytical PKMs (Kong & Gosselin, 2001), PKM dynamics (Perreira, 1999), singularity analysis of spatial PKMs (McCarthy & Hao,1998), modular parallel platforms (Zhenqun & Zhiming, 1999), PKM application for calibration of inertial measurement unit (Hall,2000) and closed form forward kinematics for especial platform structures (Selfridge & Matthew,2000).

The reason behind the popularity of parallel manipulators is their lower overall compliance (or higher stiffness) resulting in increased positional accuracy. Higher stiffness is associated to the fact that forces acting on the mechanism are transferred to the legs which are stiffer in response to compression/tension as compared to other components. The parallel distribution of legs in PKMs helps in negating the buildup of error as forces are distributed equally among the legs. In addition, certain PKM designs offer high operational speeds by mounting their actuators at base thus reducing the moving masses (Bonev,1998). But using PKMs is not always a win-win situation as they various shortcomings like low dexterity, relatively small workspace, high anisotropy and requirement of complex control due to the highly coupled dynamics. (Bonev,1998).

2. Stiffness analysis of parallel manipulators

While estimating the performance of robotic systems, one of the most important indicator is the mechanical stiffness (Park,2008; Angeles,2008; De Luca, 2008). This is the reason for which the past research and development work is targeted mainly towards the ever increasing need for higher stiffness and thus more rigid manipulators. Particularly, for industrial applications of these manipulators, where the prime objective is the accurate placement of tool, mechanism's stiffness dictates the magnitude of positioning error that may arise under the effect of external loading. In industrial pick and place applications e.g. warehouses, assembly lines etc require simple but fast manipulations. Here stiffness requirements are such that an admissible velocity/acceleration is achieved, to avoid any unwanted inertial displacements, while approaching the desired (Y. Nof,1999). On the other hand examples involving large PKMs such as being used for patient positioning in medical applications, here positioning errors are primarily caused by the

deformations in mechanical components under the effect of their own weight and payload mounted on them (Meggiolaro,2005). In all of above mentioned cases, it is desirable to keep stiffness at a higher level so that relevant system requirements can be achieved safely. Similar to general structural mechanics (Timoshenko,1970; Hjelmstad,1997), the stiffness analysis of mechanism calculates its resistance to the deformations produced as results of external force/torque acting on end-effector (Duffy,1996). This property is usually represented numerically in terms of the stiffness matrix K, which gives a linear relation between the translational/rotational displacement and static forces/torques responsible for this transition (for small quantities of all of these). The inverse of stiffness matrix (K) is compliance matrix denoted by 'k'.

The existing methodologies for modeling the stiffness of PKM's can be listed as follows:

i. Matrix Structural Analysis (MSA)
ii. Virtual Joint Method (VJM) also known as lumped modeling
iii. Finite Element Analysis (FEA)

i. Matrix Structure Analysis (MSA)

The MSA integrates the main ideas of FEA (Deblaise et. al., 2006; Martin,1996; Nagai et. al., 2008; W.Li et. al.,2002;), links are assumed to be rigid and manipulator's structure is defined using large elements and flexible beams. In this technique each compliant element is identified and stiffness matrix is developed using local coordinates which are then transformed to reference coordinate. Overall stiffness of mechanism is then calculated by assembling the stiffness matrices in reference coordinate. Computational time and expense is saved using this strategy, but a comprise has to be made on accuracy of parametric stiffness obtained as it does not provide any exact physical relationship.

Due to its constraint in accurate prediction of parametric stiffness analysis MSA has been mostly employed to determine the static stiffness of parallel manipulators. For example stiffness analysis methodology of a 6-RSS PKM is presented by Soares et. al. (2011). Author assembled the global stiffness matrix by considering joints as fixed and structure as free. Static stiffness of manipulator has been modeled to calculate the end effectors' compliant displacement when subjected to external torques and forces. Experimental results have been used for validation.

Another instance of MSA technique is adopted by (Clinton et al.,1997) for development of a static stiffness model for a Stewart platform-based milling machine. The stiffness matrix for each element has been derived first using this approach and then these individual matrices are assemble to form a system stiffness matrix.

Dynamic stiffness have also been analyzed in few works but the application is mostly restricted to mechanisms with lesser DOF such as work done by Alessandro (2012) where MSA has been used to evaluate the linear elastic dynamics of PKMs. Top plate and base are considered as rigid. Links are either modeled as rigid or flexible. When considered as flexible it can be divided into two or more bodies. Three different scenarios are analyzed to couple the bodies with the help of joints i.e. rigid-flexible, flexible-flexible and flexible-rigid. Static deformation and the natural frequencies have been calculated for a 4-DOF PKM using this method.

ii. Virtual Joint Method (VJM)

The VJM method describes the elastic deformations of the joints, links and actuators by adding the virtual joints (localized springs) to the traditional rigid model. This technique is widely employed during pre-design phase, particularly for analytical parametric analysis. At preliminary design stage, the flexibilities (both distributed and lumped) in manipulator joints are incorporated in stiffness analysis using VJM by locating localized virtual springs at joints. The Cartesian stiffness matrix is then calculated for current pose (configuration) of this compliant mechanism.

In general, using the lumped modeling technique, a minimal computational resources are required and reasonable accuracy is achieved. However, one dimensional springs are used to model the system stiffness. Thus results obtained through this technique are hypothetical as it fails to capture the coupling effects between translational and rotational. Its application is generally limited due to some other restrictions as well.

Salisbury (1980) was the first who derived mathematical relation for Cartesian stiffness matrix. He actually came up with closed form expression for calculation of this matrix for serial manipulators with an assumption that actuated joints are the locations where whole of mechanical elasticity is concentrated. Under the same assumption, Gosselin (1990) carried

forward these results to be used for parallel manipulators (assuming rigid links and perfectly working passive joints). With further advancements in this approach, effect of link elasticity was also included by augmenting the rigid beams with linear and torsional springs (Gosselin et. al.,2002). Currently various variants and simplifications of VJM exists, with slight variation in modeling assumptions and numerical techniques applied. VJM has been applied particularly to CaPAMan (Ceccarelli et. al.,2002), Orthoglide (Majou et. al.,2007; Pashkevich et. al.,2009) and H4 manipulators (Company et. al.,2002), specific designs of Stewart–Gough manipulator with US/UPS legs and other kinematic architectures (Vertechy et.al., 2007).

Fairly recent publication is of Anatol Pashkevich et al. (2011) where they have proposed a new stiffness modeling methodology for manipulators with loaded passive joints. The proposed method incorporates non-linear effects in stiffness calculation and employs VJM technique where link elasticity is incorporated through the use of 6-DOF springs. The spring parameters are calculated using FEA.. The developed methodology has been used to calculate the static stiffness of Orthoglide type parallel manipulator for four vertices of cube inside the workspace and has been able to detect non-linear behavior when subjected to loading.

iii. Finite Element Analysis (FEA)

The FEA method, over the years has established its reputation of being the most accurate and reliable, as it provides the freedom to model the links/joints with its true dimensions and shape but at the cost of high computational time (El-Khasawneh et. al.,1999; Rizk,2006; Nagai,2007; X. Hu et. al.,2007) and is usually applied at final design stage. FEA is widely used to study the structural behavior of a mechanical system.

Extensive application of FEA in the recent years, to analysis of different structural designs, owes to the fact that it is the by far the most reliable analysis technique especially in the design phase. The advancement in computational resource has significantly reduced the analysis time, thus facilitating in faster design modification decisions and optimization of new/existing designs. FEA, though not completely, is providing an alternative to product testing thus saving huge amount of capital that was previously needed during product development phase. The accuracy of FEA results augmented with experimental data can provide a strong base for even the most complex design changes.

The technique has been used extensively in research to analyze the static stiffness of parallel mechanisms and much of application areas have been restricted to lower mobility platforms such a planer mechanisms, 4-DOF mechanism, T3R1 robots etc. (Long et. al.,2003; Corradini et. al.,2004; Bouzgarrou et. al.,2004; Piras et. al.,2005). Wang et al. (2008) have employed FEA and presented a semi-analytical approach for calculating static stiffness of PKMs having complex machine frame. The PKM is divided into two sub-systems. The modeling process is implemented by: (i) modeling the stiffness of each subsystem by considering the other as rigid; (ii) using linear superposition to generate overall stiffness model. TriVariant-B (5-DOF) robot's stiffness evaluation has been evaluated using this approach. Bonnemains et. al. (2008), in their article have studied the static behavior of PKM using FEA. Model incorporates leg and joint compliances and is implemented on two architectures: Exechon-like and Tricept PKM (both having 5-DOF). Joints modeling is done considering the local behavior of the components used. Experimental testing is conducted to identify the model parameters.

Due to FEA's capability to model a system with great detail it has been widely used in the recent years to simulate the effect of complexities, which can arise due to joint contact variation, joint clearances, link flexibility etc. But the application is mostly limited to analyze the static stiffness response of PKM. Boyin et. al. (2013) have analyzed the stiffness of a novel Stewart platform-based manipulator via kinematic error model combined with **FEA**. ANSYS 12.0 workbench environment have been used for calculating joint deformation errors which are then used in model to calculate stiffness. Static stiffness of manipulator has been analyzed at three different robot poses. Aftab et al. (2012) developed an analytical method for static stiffness modeling of Haptic devices. At first a simplified model is presented considering the platform and joints as rigid and excluding the actuation system. Then detailed model has been proposed considering stiffness of both passive joints and actuation system. Hertzian contact model has been used for calculation of contact stiffness of the spherical (nominal point contact) and universal joint (nominal line contact). The bending stiffness of the universal joint is calculated by assuming that two axis act like a simply supported beam. Results for both cases have been validated by comparing them with ANSYS and experimental results for eight different positions within workspace.

Dynamic stiffness response has mostly been evaluated for Hexapods, a special 6-DOF platform, used in precision machining operations where vibration response is the primary concern. Mahoubkhan et al. (2008,2009) have presented a model for vibration analysis of hexapod table and vibration behavior of moving platform during machining operation is of main concern. Parameters such as mass, stiffness, damping and inertia of the hexapod's elements (including the joints) have been taken into account. Only upper platform is considered rigid rest all are modeled as flexible elements. The Eigen-value problem has been used to obtain modal frequencies for ten different configurations and analytical results have been evaluated by comparing them with FEM results. The operating frequencies are high as table is subjected to machining operations.

3. Joints & mechanical stiffness of manipulators

Joints play an important role in mechanical stiffness of parallel robots. In most of research, joints are considered as rigid with constant stiffness value. To achieve more realistic results complex effects such as joint stiffness must be incorporated in the stiffness analysis of parallel manipulators as they also play a part in degrading the positioning accuracy.

Zili Zhou et al. (2010) have presented model for flexible joint of a PRS parallel manipulator that depends on its configuration. The variation in joint looseness with change in system's configuration causes joint flexibility and has been simulated by adapting virtual springs between the joint components. Parameters for flexible joints are set using the dynamic characteristics of system and are obtained by conducting experimental modal testing for a selected set of robot configurations. Results showed a good agreement between calculated and measured mode shapes. Carlo et al. (2011) has discussed a 3D model of a revolute joint (having clearances) which poses force constraint (perfect joint imposes kinematic constraints). Four different contact scenarios i.e. one point, two point (both in and out of plane) and line contact have been evaluated using FEA to determine the stiffness parameters. The dynamic behavior prediction of industrial manipulator is improved by adopting proposed technique.

4. Optimization

Over the years optimization techniques have been extensively applied to PKMs for optimum configuration of joints, link lengths, work space optimization, compact and light weight designs etc. Most of this work is based on the traditional optimization techniques. These techniques, however, fail to converge to a true solution when handling a problem involving large number of geometric variables. Many researchers have seeked an optimum design for various robotic manipulators (Bergamaschi et al, 2006; Rout & Mittal, 2008; Miller & Stock, 2003; Ceccarelli et. al., 2004). Lum et al. (2006) have come up with an kinematic optimization technique that enables the design of compact and light weight surgical manipulator with smallest possible configuration. Chablat (Chablat & Angeles, 2002) have employed Jacobian matrix to reach an optimum size for revolute-coupled planar manipulators. Jacobian distances are compared with given isotropic matrix to be further used as reference model. Link length of spatial PKM have been optimized by Zhao et al. (2007) using the method of least variables. Boeij et al. (2008) worked on optimization of a contactless electromagnetic 6-DOF actuator using sequential quadratic programming method. Xinjun LIU et al. (2011) have designed two rigid links of a PKM by employing the techniques of topology and size optimization. Development of structures with minimum weight but maximum rigidity has been optimization criteria. A new optimal algorithm called the Guide-Weight method is introduced for carrying out topology optimization. Results of topology optimization have been used to design the applicable structures of the rigid links. Size optimization is performed using the commercial software ANSYS in order to model the structures parametrically and to optimize these parameters.

Evolutionary optimization methods, i.e. genetic algorithms (GA), as compared to traditional techniques can find global optima as they use stochastic search methods, thus eliminating the problem of sticking to local optima (Holland, 1975). Thus the optimization using the evolutionary methods has proved as an effective solution. António et. al. (2012) have used neural network and genetic algorithm to optimize the kinematic design of 6-DOF PKM where maximum dexterity is set as an objective function.

5. Motivation

Although a lot of research has been carried out to analyze the stiffness behavior of parallel platforms but after reviewing the work done to date it is evident that there are certain gaps in application of FEA to stiffness analysis of PKM's. This includes the scarcity of its implementation to determine the dynamic stiffness response, especially for large heavily loaded 6-DOF platforms (space launch, military applications, motion simulators etc). A research gap exists and a need is felt to develop an accurate modeling and simulation technique for application of FEA, so that a better match between FEA and experimental results could be obtained, for such parallel mechanisms.

Most of work reviewed lays primary emphasis on work space analysis, active/passive joint contacts/clearances, link flexibility effect on static stiffness of PKMs in terms of deformation/ displacement. The top plate stiffness behavior greatly dominates the overall stiffness characteristics of large mechanisms subjected to heavy loads. The absence of incorporation of top plate structure design in overall system modeling and analysis questions the accuracy of overall stiffness of these PKMs.

Moreover, joints also play an important role in degrading the positional accuracy, thus complex effects i.e. joint stiffness must also be incorporated in model to achieve more realistic stiffness results. Most commonly used strategy for modeling joint flexibility (as seen in literature) is to consider joint stiffness constant and is applied for active joints only. In most of existing FEA based methods if joints behavior is ignored by considering their stiffness constant, it could result in

i. Overdesign that compromises the performance
ii. Excessive deflections
iii. Can even encounter failure in terms of vibration or strength

This necessitates the investigation of effect of joint contact condition on the overall stiffness (both static and dynamic) behavior of top plate. This includes the selection of suitable joint boundary condition in order to reach a design that will behave the same way when tested experimentally as predicted in simulation results.

Lastly as for large heavily loaded manipulators, top plate shares a major percentage of the cumulative mechanism's weight. For increased dynamic performances it is imperative to have a light weight design using small actuators which operates at lesser power level (energy efficient). So an optimization study is required for top plate to reach a lightweight design while keeping the desired stiffness of top plate.

6. Objectives

Thus the objectives of this work relates to following different aspects of top plate

i. Stiffness behavior analysis of 6-DOF platforms' top plate subjected to various joint boundary conditions under heavy loading.
ii. Multi objective structural optimization of top plate to achieve weight optimum design matching experimental results.
iii. An optimum design which is stiffer against deflections and presents higher frequency ranges to avoid vibrations.

CHAPTER 3

MODELING AND METHODOLOGY

A methodical procedure is presented in this section for analyzing the overall stiffness characteristics of heavily loaded manipulator's top plate under different joint and loading conditions. The evaluation of the results was concluded via physical experiments. Further refinement in the analysis procedure was done to minimize the deviation from experimental results. The methodology adopted to carry out the research work is presented in the form of flow chart in Figure 3. The brief description of each step involved is given in the next sections.

1. Top plate design

Top plate design is of prime importance if operational accuracy and safe working of the system is to be ensured. The main emphasis of this analysis is to optimize the dynamic response of the top plate. Thus the objective is to design a light weight structure with maximum frequency. The broad requirements for which the top plate of parallel platform is designed are summarized in Table I.

Payload capacity	20 ton
Motion Requirements	$\pm 30^{o}$ tilt (global x, y and z axis)
Frequency	3.0 Hz
Minimum deflection	4.0 mm
Acceleration	2.5g
Factor of safety	3.0
Platform Shape	Triangular

Table 1. Broad requirements for top plate design

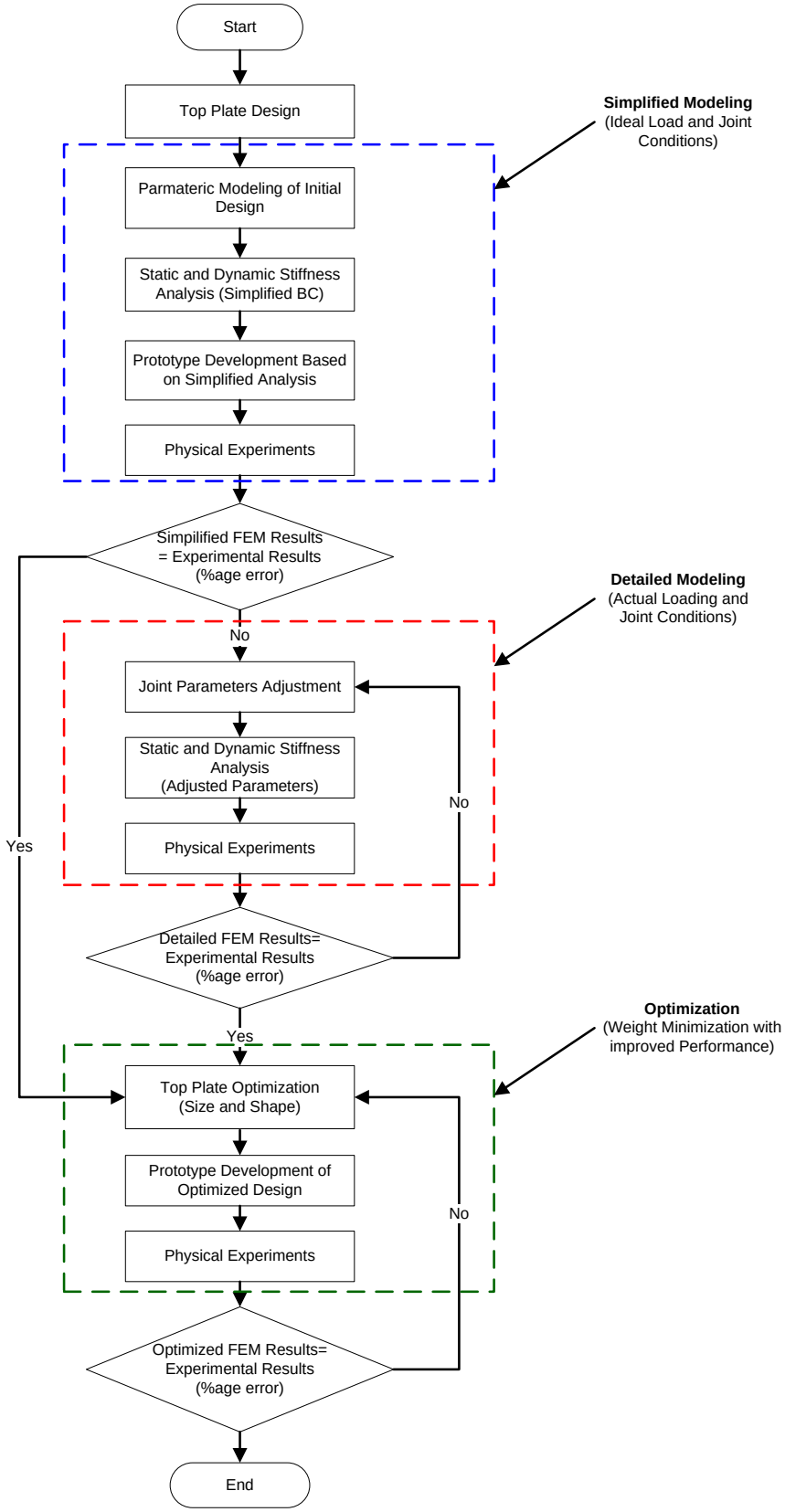

Figure 3. Methodology flow chart

Irregular hexagon shape is considered for top plate design. Three joint attachment points are located at an angle of 120^{o} along the three small sides to control the platform's 6-DOF motion. Joint attachments with the top plate are modeled as rectangular cavity in order to keep the stiffness analysis simple for simulating the joint contact conditions. A hollow rib patterned top plate structure is used in order to fulfill the objective of light weight design. The shape of top plate to be designed and joint attachment points are depicted in Figure 4 and Figure 5.

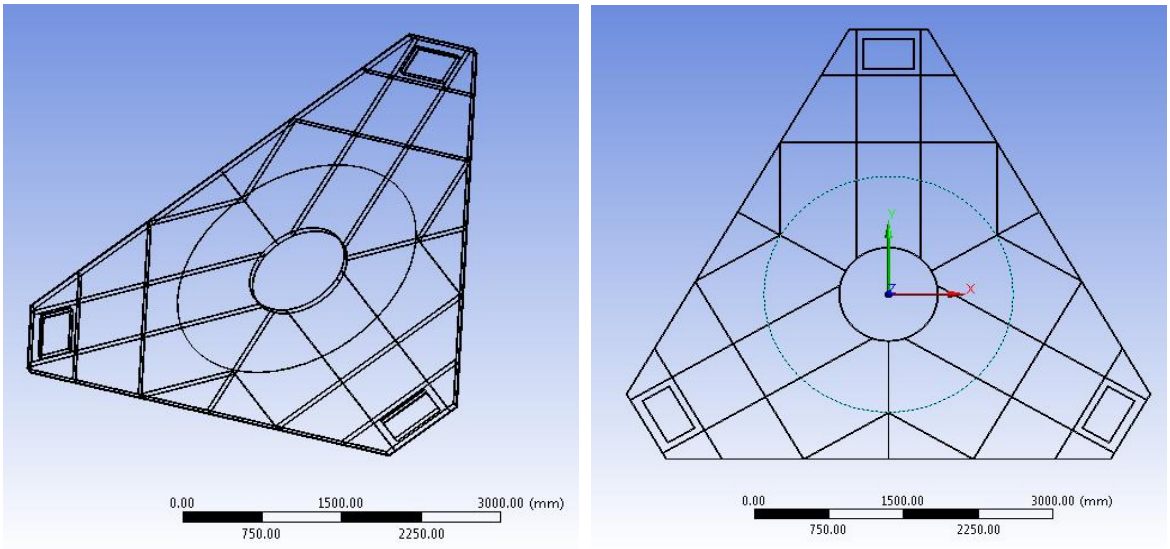

Figure 4. Top plate shape and rib structure used

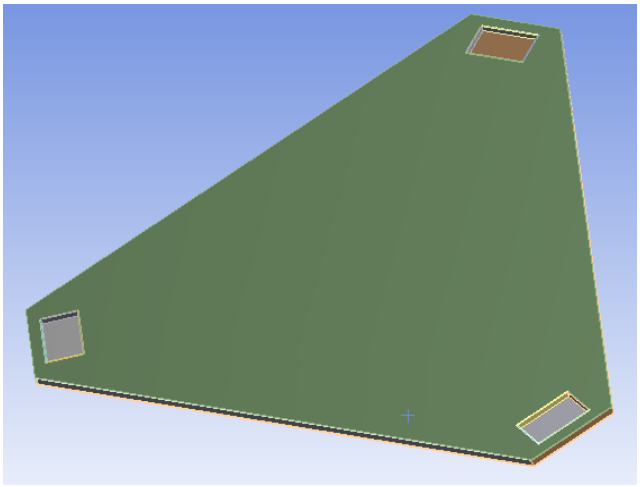

Figure 5. Geometry used for simulating joint attachment.

2. Simplified modeling

In the simplified modeling stage it is assumed that joints are rigidly attached with the top plate on which task load is mounted and thus contact stiffness of joints is ignored. Load is applied in order to analyze the stiffness behavior of top plate under the weight of the payload. The approach used can be summarized as follows.

i. Parametric Modeling of Initial Design

Top plate is designed using these simplified assumptions. The parametric modeling of finalized structure is then done using a solid modeling tool. This in turn gave a simplified model to be further used for FEM analysis which is followed by prototype development and experimental testing for stiffness evaluation.

ii. Simplified FEM Modeling

In this step, stiffness of joints is ignored by considering them to be rigid i.e. complete volume of joint is making contact with top plate in order to support the load.

Moreover in order to simulate the effects of 20 ton task load, actual load is modeled (shown in Figure 6. Both static and dynamic stiffness behavior of top plate is analyzed for this contact type.

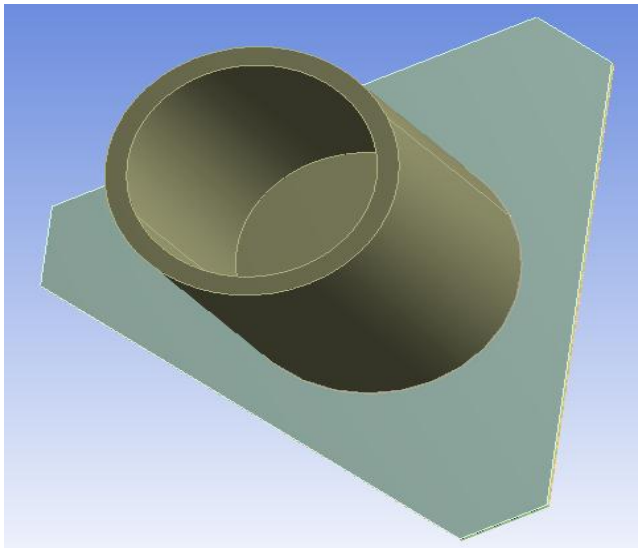

Figure 6. Load applied to simulate payload

iii. Prototype Development and Physical Experiments

To complement and validate the results from FEM models, the following structured physical experiment is proposed.

a) Prototype of top plate is developed based on the design using simplified modeling.
b) Top plate is assembled with the joints to complete the 6-DOF mechanism.
c) Actual loading is applied and the static deflection is noted.
d) Mechanism is tested for operating conditions to calculate the fundamental resonant frequency.

iv. Evaluation of Simplified Results

Simplified physical experiment is set up to verify the results obtained through FEA model. The deviation from the experimental results would ascertain the amount of accuracy to which the model is implemented to the problem. Improvement in the procedure adopted, if any, is to be made by taking into account percentage relative error criterion.

3. Detailed Modeling

In the detailed model, the contact stiffness of joints is incorporated by simulating different type of contacts that joints can make with top plate. Actual load is modeled to analyze the stiffness behavior of top plate with the payload. The approach used can be summarized as follows.

i. Detailed FEM Modeling

In detailed FEM modeling, actual payload is modeled and applied on the top plate geometry in order to simulate the actual loading conditions. The details of task load modeled are given in Table 2.

The nominal area contact and line contact conditions are proposed to calculate the contact stiffness of joints, respectively. The static and dynamic stiffness behavior of top plate is analyzed for these two joint contact conditions.

Weight	20 ton
Diameter	2.5 m
Height	6.0 m
C.G.	2.0 m from base
Mass moment of inertias	
Ixx	6.12×10^7 t·mm²
Iyy	2.33×10^7 t·mm²
Izz	6.12×10^7 t·mm²

Table 2. Task load specifications

ii. Physical Experiments

In the detailed physical experiment, the complete system is experimentally tested. The steps proposed for the simplified physical experiments can also be used to perform these tests. Evaluation of detailed results

A similar procedure, as used for simplified modeling, is adopted to verify the detailed modeling results i.e. results from a detailed physical experiment are correlated with the detailed analysis results to determine their accuracy. The same criterion of percentage relative error is used for this instance to find the deviation from actual results.

4. Top plate optimization

Once the correct boundary conditions have been identified and stiffness parameters of initial design of top plate have been validated using the experimental results. The structure of top plate is optimized to have desired stiffness characteristics with the minimum overall weight. For this purpose a two step approach is proposed

a) Size of top plate is optimized to achieve the desired static and dynamic stiffness characteristics.
b) Shape of top plate is optimized in order to have a structure with minimum possible mass while satisfying the desired stiffness requirements.

For carrying out this work a goal driven optimization study on top plate has been carried out using ANSYS design exploration module. It employs design of experiments (DOE) technique in order to determine the response of component for variation in given input parameters. Then optimization techniques, i.e. screening, multi-objective GA, are employed on the generated search space in order to determine the best design meeting the desired objectives and constraints.

i. Size Optimization

In size optimization the overall height and rib thickness of top plate are chosen as design variables to be optimized for having desired static and dynamic stiffness of top plate under the effect of constant payload. The minimum weight is used as constraint in this step. In order to carry out this optimization two parameters were created to drive the whole top plate assembly

DS_height: representing the height of each rib been used in the structure and thus controlling the overall height of top plate (Figure 7)

DS_width: representing the thickness of each rib, width of the upper plate and lower plate in the top plate assembly (Figure 7)

Thus **the total height of top plate = DS_height + 2*DS_width**

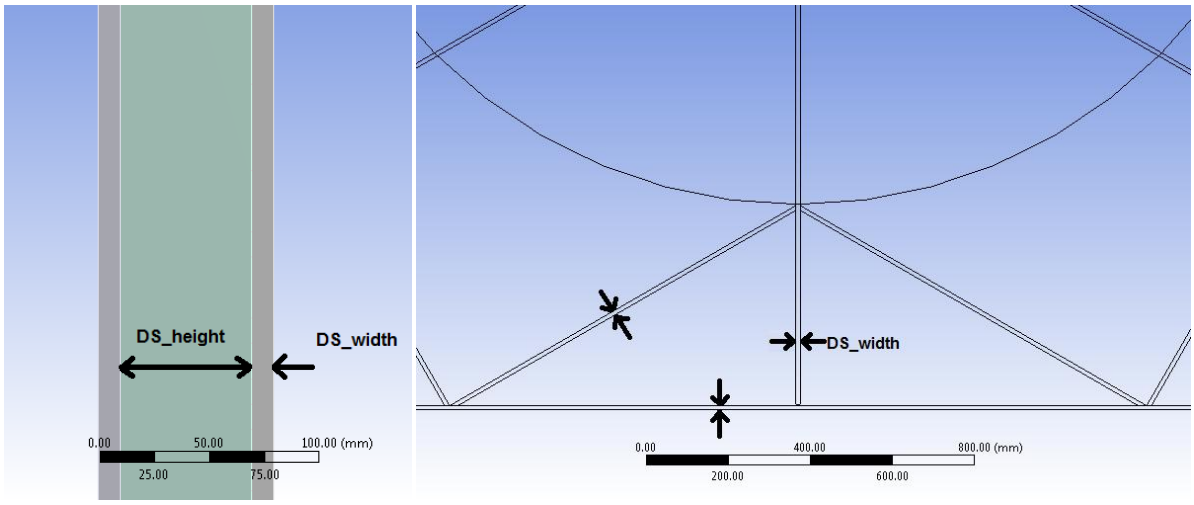

Figure 7. Height and width parameters used for controlling top plate assembly

ii. Shape Optimization

After having optimized the overall height and rib thickness of top plate. Shape of the top plate is optimized with the objective of having a light weight structure with minimum possible

weight. For this purpose the structure height at centre is kept fixed while height at outer section is optimized for weight reduction. The optimized structure thus bear desired static and dynamic stiffness behavior but with the minimum possible mass. In order to carry out this optimization three parameters were created to drive the whole top plate assembly

DS_total_height: representing the height of ribs of top plate at centre section carrying the payload (Figure 8).

DS_outside_height: representing the height of each rib at outer section including the joints cavity (Figure 8).

DS_width: representing the thickness of each rib, width of the upper plate and lower plate in the top plate assembly (Figure 8).

Thus

Total height of top plate at centre = DS_total_height + 2*DS_width

Total height of top plate at outer section = DS_outside_height + 2*DS_width

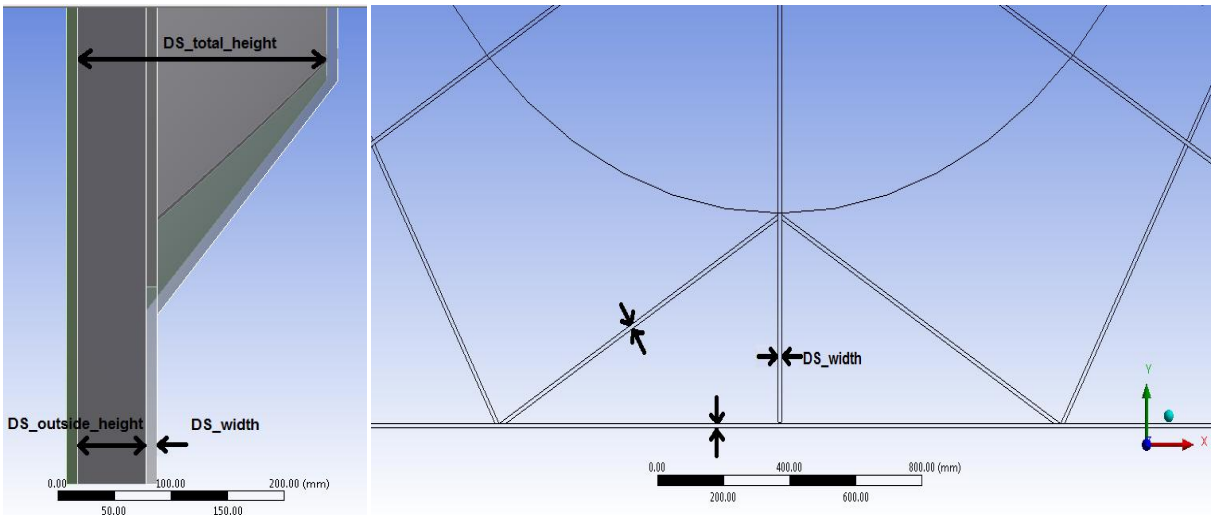

Figure 8. Height and width parameters used for controlling Top plate assembly

iii. Prototype Development and Physical Experiments

A prototype of top plate based on the results of the optimized design is developed. The experimental testing is performed on this design and the actual stiffness response of the optimized structure is determined.

iv. Evaluation of Optimized Results

The same procedure is adopted to verify the results of optimization as adopted for detailed modeling. The FEM results are correlated with experimental results. A validation criterion based on percentage relative error is used to validate the simulation results.

CHAPTER 4

BOUNDARY CONDITIONS EFFECT ANALYSIS

Static stiffness results were evaluated in terms of total deformation of the top plate while the dynamic response was measured in terms of modal frequencies. The first modal frequency is of prime interest as it is the lowest frequency at which the structure would resonate when subjected to operating conditions, so the result evaluation was primarily based on checking the first modal frequency.

As the factor of safety (FOS) for the current design is set to 3.0, it corresponds to a minimum 1st modal frequency of 9.0 Hz while keeping the static deformation within the allowable limit of 4mm for final design of structure.

1. Top plate design

For initial design of top plate the free modal analysis was conducted using the ANSYS workbench environment in order to determine the 1st natural frequency of top plate while static deformation of top plate under its own weight was calculated. The top plate is designed in following steps.

i. Geometric shape selection
ii. Circumscribed diameter specification
iii. Identification of joint location points
iv. Material selection
v. Determining the thickness/height of top plate based on static & modal analysis

Rib patterned structure was used to design the top plate in order to achieve the objective of light weight design. For this purpose various rib patterns were considered. Static and modal analysis were conducted for each structure until a design is achieved which deforms and vibrate in the same way as solid top plate. The material used is structural steel whose properties are given in Table 3.

Density	7850 kg/m^3
Elastic Modulus	200 GPa
Poisson Ratio	0.3
Tensile Yield Strength	0.25 GPa

Table 3. Material properties of Structural Steel

The results for static and modal analysis were obtained considering the ideal joint behavior , i.e. rigid, which is a standard practice for designing such structures. The 1st natural frequency obtained was 21.03 Hz which is approximately seven times the operating frequency while total deformation is less than 1mm (Table 4). The static deformation and 1st mode shape contours are shown in Figures 9 & 10. As the results obtained are meeting the objectives set in terms of FOS, so this design was selected for further evaluation of its stiffness behavior under loaded mode. The specifications of top plate design finalized for further evaluation are given in Table 5.

Static total deformation (mm)	0.7638
1st Natural frequency (Hz)	21.036

Table 4. Stiffness response of initial design of top plate

Top plate mass (ton)	2.64
Top plate height (mm)	80
Rib Thickness (mm)	10
Upper & Lower plate thickness (mm)	10
Length of longer side (mm)	4460
Length of shorter side (mm)	800
Circumscribed diameter (mm)	7000
Circular rib diameter (mm)	1000
Joint attachment geometry (mm^3)	500 x 300 x 50

Table 5. Specification of initial design of top plate

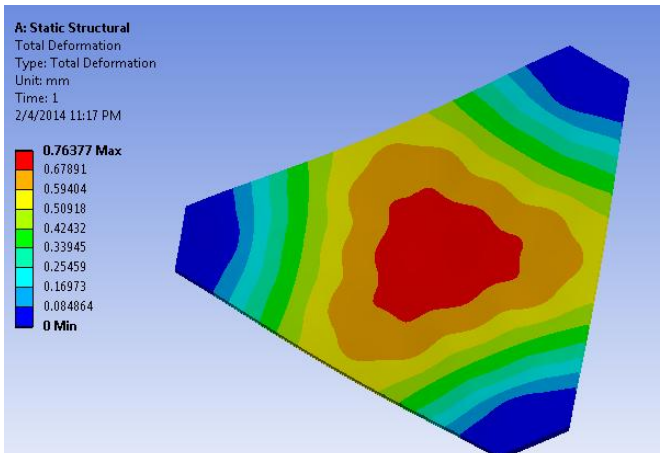

Figure 9. Static total deformation for initial design of top plate

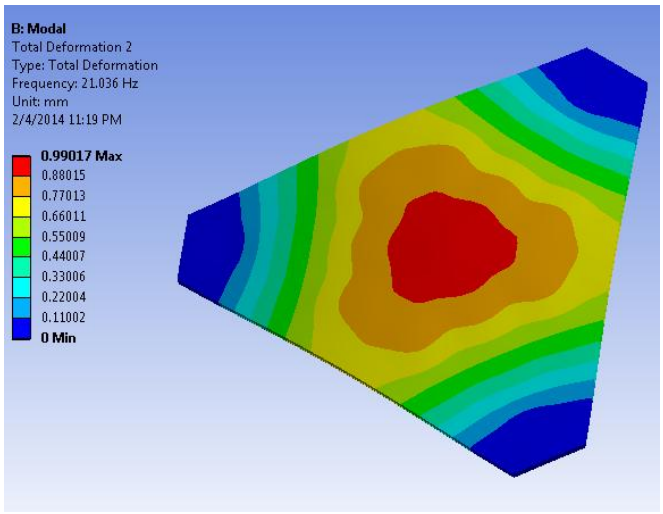

Figure 10. 1st Mode shape contours initial design for top plate

2. Simplified modeling

To apply the proposed analysis methodology to the structure, a parametric model of top plate designed was generated according to the specifications presented in Table 5.

i. FEM Results

FEA based results were obtained using ANSYS workbench and are presented in this section. The static deformation obtained is 4.24 mm (Table 6) and 1st modal frequency is 4.36Hz (Table 7). Static total deformation contours are shown in figure 11, while mode shapes for first three frequencies are shown in figure 12-14.

Static total deformation (mm)	4.2379

Table 6. Static stiffness results for simplified FEM model

Mode	Frequency (Hz)
1st	4.3637
2nd	4.3744
3rd	7.7538
4th	101.69
5th	102.30
6th	102.80

Table 7. Dynamic stiffness results for simplified FEM model

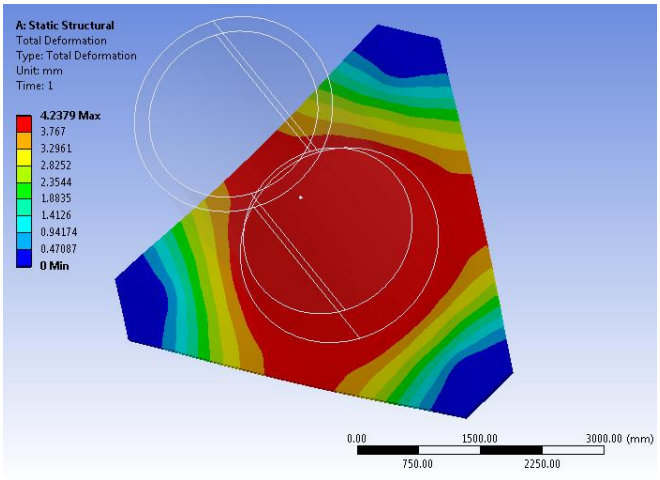

Figure 11. Static total deformation contours (simplified FEM)

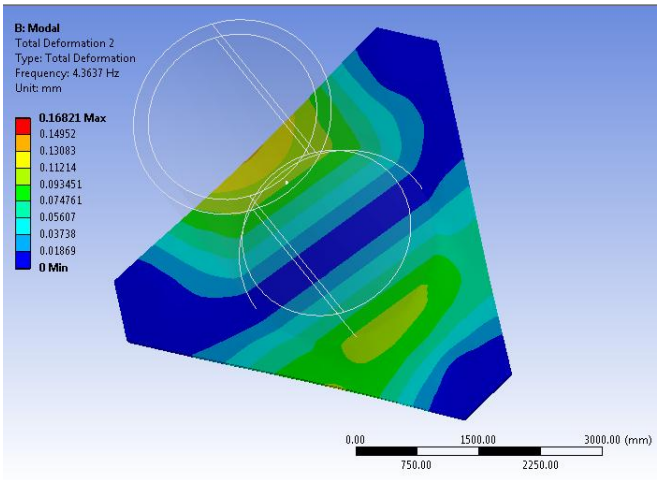

Figure 12. Mode shape for 1st mode frequency (simplified FEM)

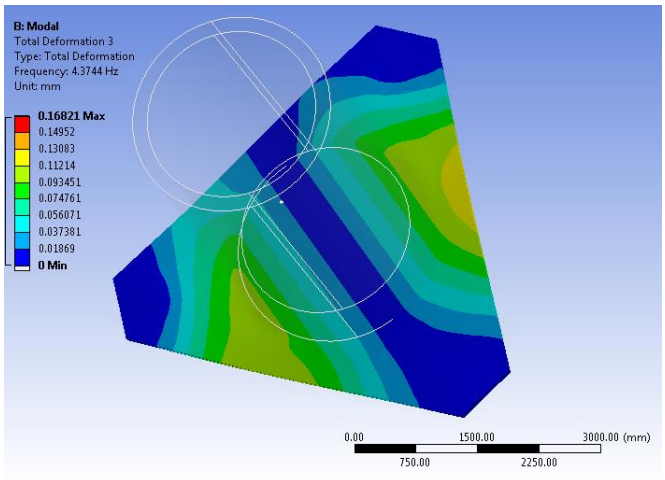

Figure 13. Mode shape for 2nd mode frequency (simplified FEM)

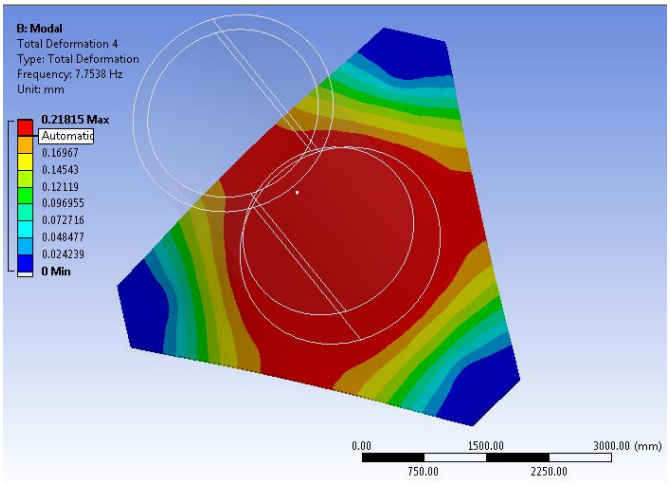

Figure 14. Mode shape for 3rd mode frequency (simplified FEM)

ii. Experimental Setup

To validate the results from FEM model, a physical prototype of the selected test case was developed and tested experimentally.

A set of guidelines, how to experimentally evaluate the stiffness parameters are presented here. The stiffness measuring method requires common metrology devices, such as a dial indicator with resolution of 0.01 mm, a vernier caliper and weights. These were calibrated and specified according to standards. Their working temperature range is [-10^{o}C, 60^{o}C]. Approximate test conditions were, 1 atm pressure and 25^{o}C temperature.

The structure started to resonate when tested for operating conditions and results obtained for static deformation and 1st modal frequency during experimental testing are presented in Table 8.

	P0	P1	P2	P3	P4	Avg. Value
Static (mm)	12.8	12.8	13.6	13.9	12.7	13.2
1st Modal (Hz)	2.8	2.7	2.7	3.0	3.2	2.88

Table 8. Experimental values for top plate designed (pre-optimized)

iii. Results Correlation and Evaluation

To validate the results obtained from simplified FEM modeling, they were compared with the results obtained through experiments and are shown in Table 9. The maximum relative error for 1st modal frequency is 61.5% while average relative error is 52.1%. Similarly the maximum relative error for static deformation is 69.5% and average value is 67.7%. The percentage error was beyond the acceptable range, which motivated the development of a more detailed model.

	P0	P1	P2	P3	P4	Avg. Value
Static (%)	66.9	66.9	68.8	69.5	66.6	67.7
1st Modal (%)	55.7	61.5	61.5	45.3	36.3	52.1

Table 9. Relative error between experimental & simplified FEA results

3. Detailed Modeling

An iterative procedure was adopted in which joint contact conditions were changed systematically until a desired accuracy is obtained between the FEM results and experimental results.

i. Area Contact Analysis Results

Results obtained considering the area contact between joints and top plate is presented in this section. The static deformation obtained is 5.04 mm (Table 10) and 1st modal frequency is 4.20Hz (Table 11). Results show that 1st mode frequency has dropped as compared to rigid joint condition; moving more closer to experimental results. Similarly static deformation value has increased.

ii. Line Contact Analysis Results

In order to get more accurate results another contact condition i.e. one line of joint making contact with top plate is considered and results for this case are presented in Table 10 & 11. The results obtained depict a sharp increase in the static deformation from 5mm to 12.63mm and drop in resonant frequency from 4.2 Hz to 3.143 Hz. The static deformation contours and first three mode shapes using line contact scenario are shown in figure 15-18.

	Area joint contact	**Line joint contact**
Static total deformation (mm)	5.0465	12.63

Table 10. Static stiffness results for detailed FEM modeling

Mode	**Frequency (Hz)**	
	Area joint contact	**Line joint contact**
1st	**4.2012**	**3.134**
2nd	4.2125	3.326
3rd	7.1012	4.4767
4th	99.805	76.227
5th	100.37	78.829
6th	101.18	92.276

Table 11. Dynamic stiffness results for detailed FEM modeling

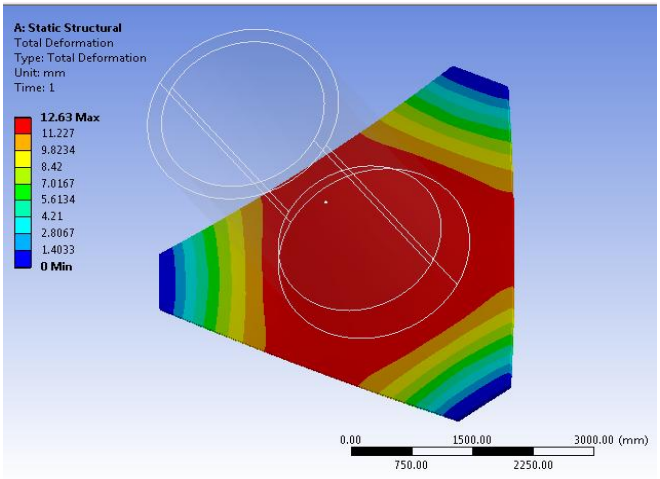

Figure 15. Static total deformation contours (detailed FEM)

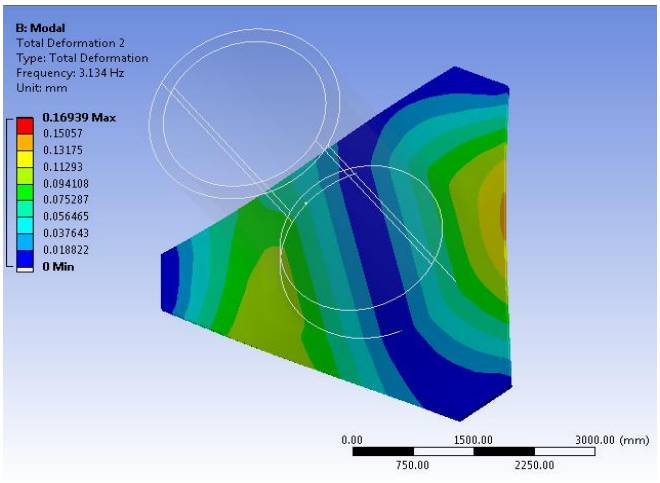

Figure 16. Mode shape for 1st mode frequency (detailed FEM)

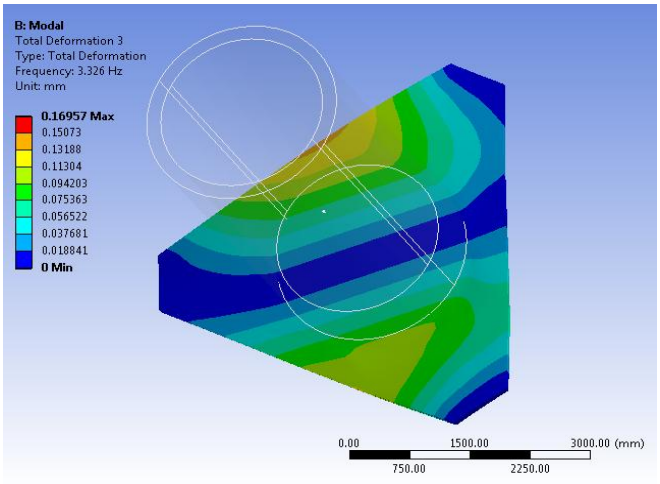

Figure 17. Mode shape for 2nd mode frequency (detailed FEM)

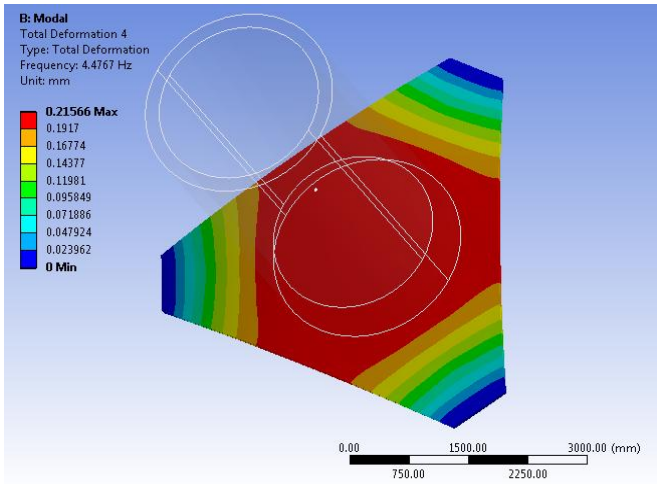

Figure 18. Mode shape for 3rd mode frequency (detailed FEM)

iii. Results Correlation and Evaluation

The results from detailed FEM modeling were compared with the experimental results in order to validate their accuracy in predicting the actual behavior and are shown in Table 12.

The maximum relative error for 1st modal frequency using area joint contact condition is 55.6% while average relative error is 46.5%. The deviation from the experimental results for this scenario is more than acceptable value.

For line contact condition the maximum relative error obtained for 1st modal frequency is 13.7% and average relative error is 8.7%. The errors for this case are within acceptable range. Thus no further joint condition needs to be analyzed.

		P0	P1	P2	P3	P4	Avg. Value
Area Joint Contact	**Static (%)**	60.5	60.5	62.9	63.6	60.2	61.5
	1st Modal (%)	50.0	55.6	55.6	40.0	31.3	46.5
Line Joint Contact	**Static (%)**	1.30	1.30	7.10	9.10	0.60	3.90
	1st Modal (%)	11.0	13.7	13.7	4.30	2.20	8.70

Table 12. Relative error between experimental & detailed FEA results

Figure 19-20 compare the average experimental value with variation of static total deformation and resonant frequency for three joint contact conditions considered. By looking at these figures it could be ratiocinated that the line contact condition gives a more realistic prediction of overall stiffness behavior for the top plate and thus is best condition to be applied in order to design a top plate.

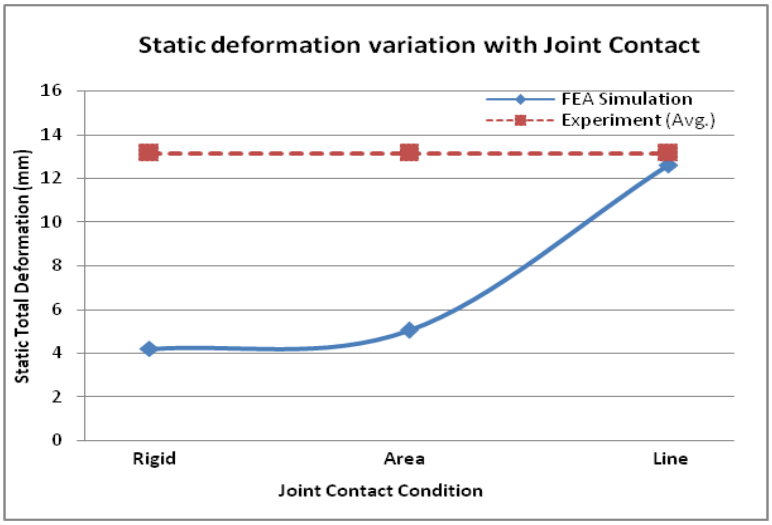

Figure 19. Static deformation variation with joint contact

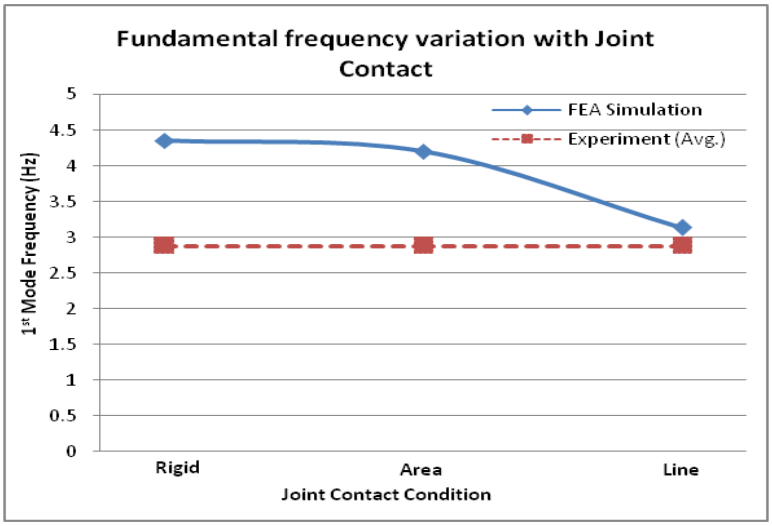

Figure 20. 1st mode frequency variation with joint contact

CHAPTER 5

TOP PLATE OPTIMIZATION

The initial design of top plate failed to give the desired performance once the correct boundary condition for joints were identified. Thus the top plate needs to be redesigned using the correct boundary condition. In order to achieve this purpose a goal driven optimization study on top plate was carried out using ANSYS design exploration module and the results are presented in this chapter.

Design of experiments (DOE) technique was employed to generate the design space to be further used for optimization. Response surface methodology was used to generate response surface of component for variation in given input (design) parameters. Central composite design technique was used for DOE and values of design variables were generated using face centered (enhanced) method. Full 2^{nd} order polynomial method was applied for creating response curves/surfaces for these values of design variables. Finally two optimization techniques i.e. screening and MOGA were employed in order to obtain optimum candidates within generated search space. At the end the best design meeting the desired objectives and constraints was selected.

1. Size optimization

The first step in optimization procedure was to optimize size of top plate so that design provides the best possible performance meeting the desired objectives with minimum possible mass. For this purpose the cross sectional area of ribs was optimized (figure 21). Thus the two design variables for the optimization problem are rib height and rib thickness respectively.

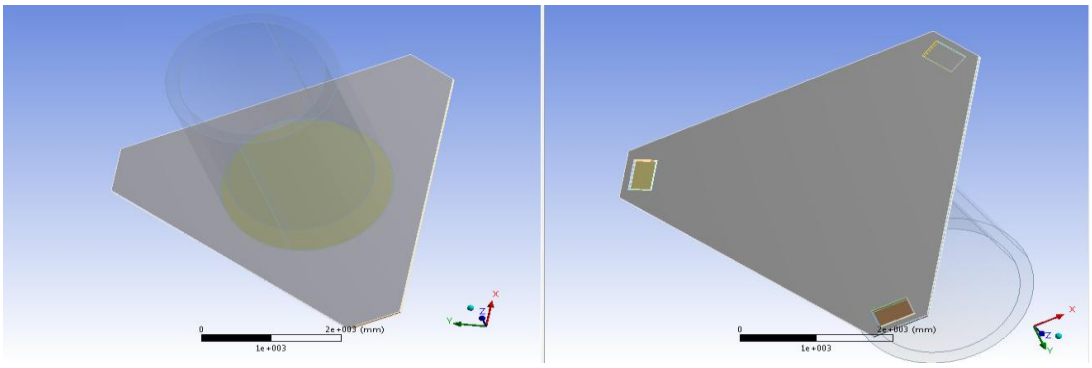

Figure 21. Top plate structure used for size optimization

The overall height of top plate is given by:

Overall height of top plate = rib height + 2*rib thickness

The optimization problem thus can be formulated as

Objectives:

Maximize	Frequency (Hz)
Minimize	Total Deformation (mm)
Minimize	Top plate mass (ton)

Constraints:

$80 \leq$ Rib Height (mm) ≤ 220

$8 \leq$ Rib Thickness (mm) ≤ 16

i. DOE Matrix

DOE matrix used for input parameters and results of mass, static total deformation and 1st mode frequency are shown in figure 22.

Table of Schematic D2: Design of Experiments (Central Composite Design : Face-Centered : Enhanced)

	A	B	C	D	E	H
1	Name	P74 - DS_HEIGHT	P75 - DS_WIDTH	P4 - Total Deformation Maximum (mm)	P7 - Total Deformation Reported Frequency (Hz)	P79 - Top Plate Mass (tonne)
2	1	140	12	3.3051	6.744	3.5844
3	2	60	12	9.9676	3.7658	3.1531
4	3	100	12	5.0869	5.3579	3.3688
5	4	220	12	2.0468	8.8905	4.0156
6	5	180	12	2.4548	7.9224	3.8
7	6	140	8	5.1103	5.4256	2.4208
8	7	140	10	4.1325	6.0501	3.0028
9	8	140	16	2.3558	7.9889	4.7465
10	9	140	14	2.7756	7.3547	4.1656
11	10	60	8	16.402	2.9497	2.1222
12	11	100	10	6.2861	4.8252	2.8203
13	12	220	8	3.0739	7.2192	2.7195
14	13	180	10	3.0443	7.1684	3.1853
15	14	60	16	6.6875	4.6058	4.1834
16	15	100	14	4.2209	5.8665	3.917
17	16	220	16	1.494	10.441	5.3095
18	17	180	14	2.1175	8.5884	4.4142

Figure 22. DOE matrix used and results obtained for objectives

ii. Response Surface

The response surface generated as a result of DOE was used as a design space for carrying out the optimization. The 3D response curves of 1st modal frequency, static deformation and top plate mass against the design variables are shown in figures 23-25. Figures 26-28 show the response of all these three objectives with variation in height of structure and thickness of ribs individually. The 1st resonant frequency varies almost linearly with the increase in top plate

height and rib thickness but is more sensitive to height of structure. The static total deformation decreases as top height and rib thickness is increased. But this decrease is elliptical with height becoming almost constant at higher values and linear with thickness. There is a linear increase in top plate mass with the increase in the values of design variables.

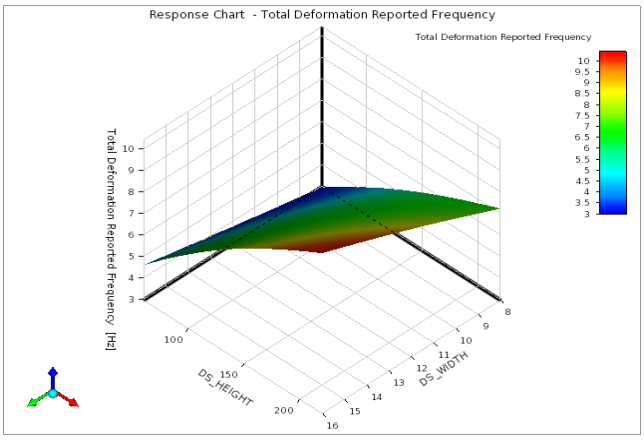

Figure 23. 1st mode frequency response against design parameters

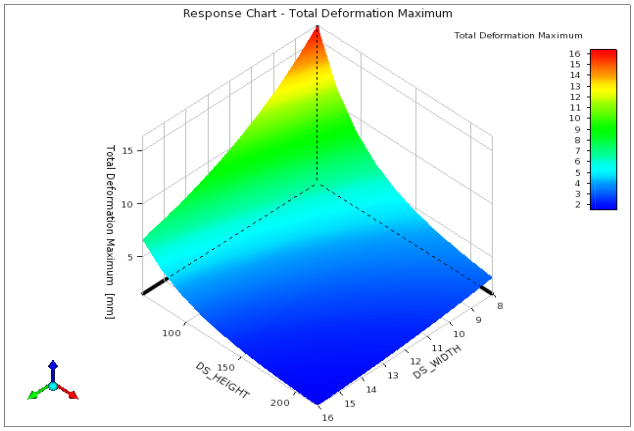

Figure 24. Static deformation response against design parameters

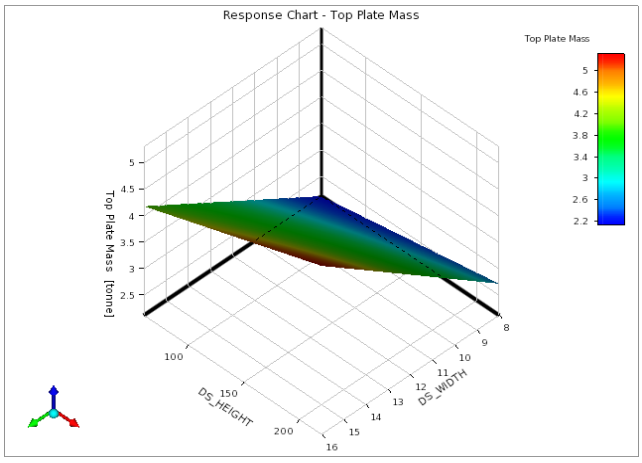

Figure 25. Top plate mass response against design parameters

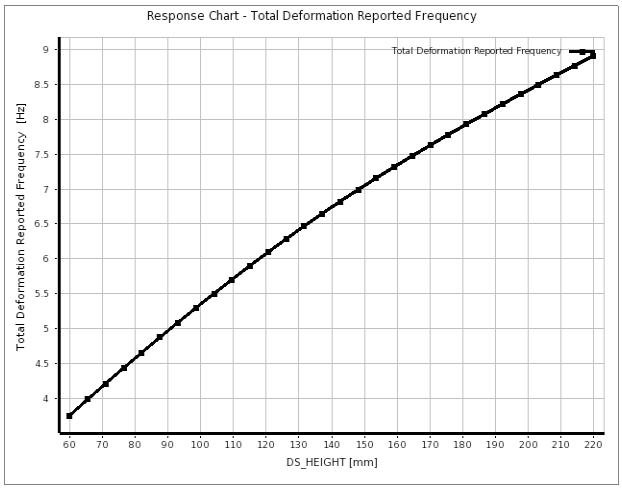

(a) DS_height parameter

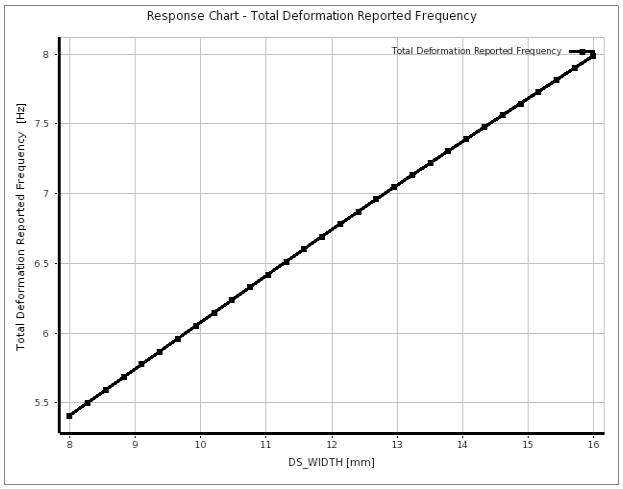

(b) DS_width parameter

Figure 26. 1st mode Frequency (Hz) response

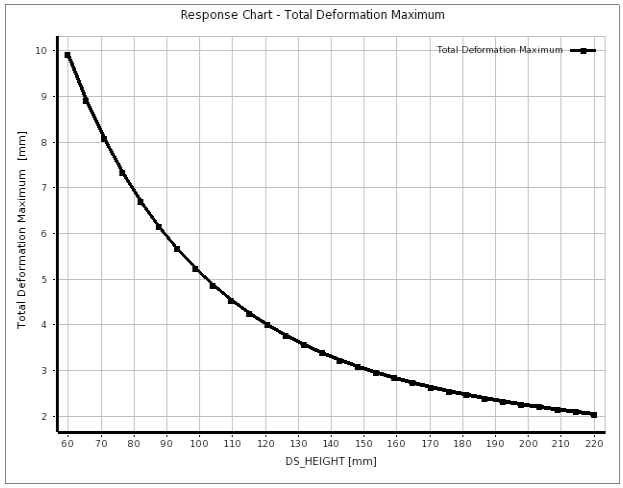

(a) DS_height parameter

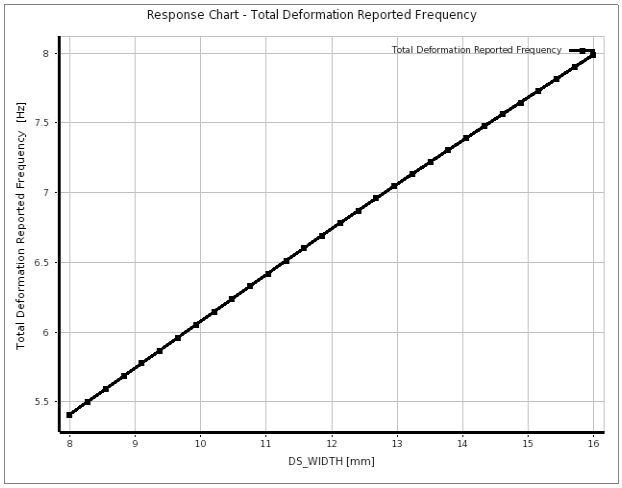

(b) DS_width parameter

Figure 27. Static total deformation (mm) variation

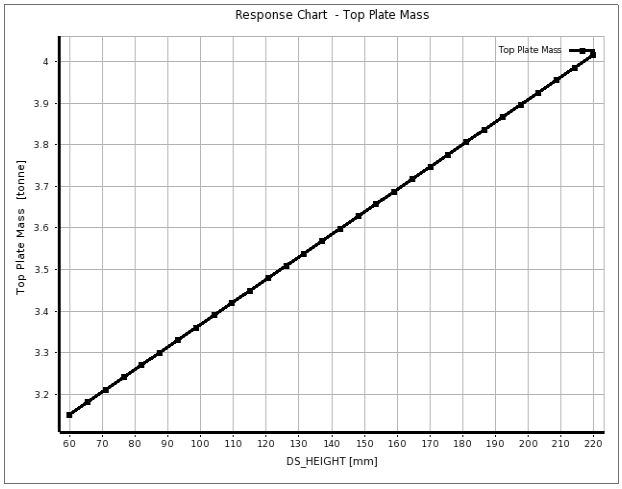

(a) DS_height parameter

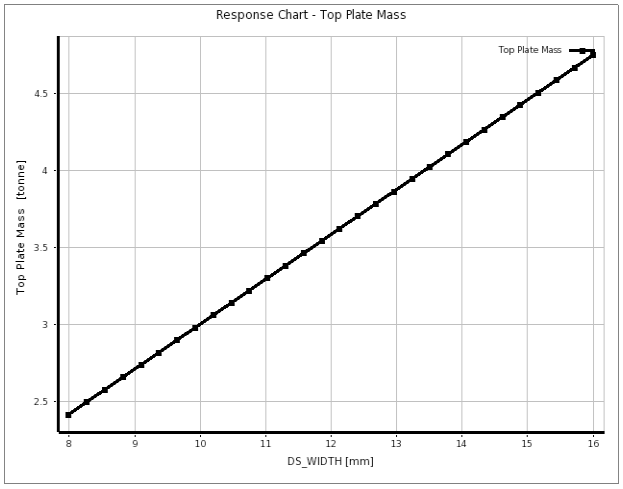

(b) DS_width parameter

Figure 28. Top plate mass (ton) response

iii. Sensitivity Analysis

Sensitivity analysis was performed after generation of response curves in order to quantify the variation of desired objectives with the design variables and determine which variable i.e. top height or rib thickness is more critical in achieving the desired objectives.

Bar graph of the sensitivities of three objectives set for carrying out the size optimization with variation in the design variables are shown in figure 29. It is evident from the chart that 1st mode frequency and maximum total deformation of top plate are much more sensitive to variation in structure's height as compared to rib thickness while mass of top plate increases more with the increase in rib thickness. Based on the sensitivity analysis height of structure of needs to be increased more compared to rib thickness.

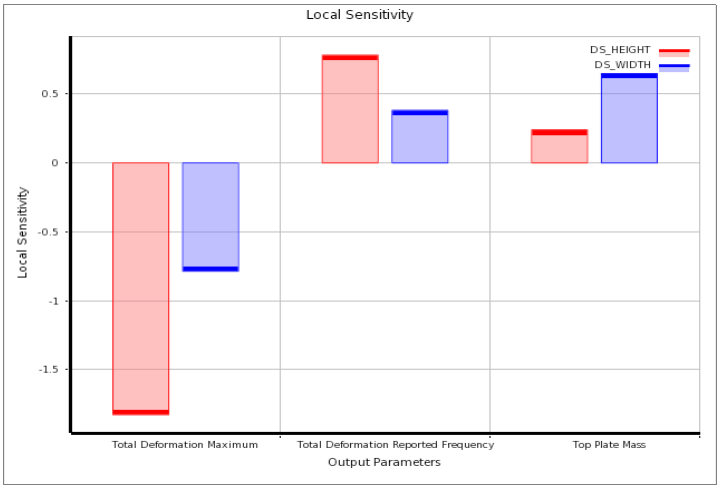

Figure 29. Local Sensitivity of output parameters with variation in input parameters

As the objective of size optimization was to design a structure with maximum stiffness while keeping the mass to minimum. Local sensitivity curves of top plate mass against the 1st modal frequency and static deformation for variation in design variables are shown in figure 30(a) & 30 (b). These curves are again suggesting that the height of top plate to be increased in greater proportion in order to have light weight design with maximum stiffness characteristics.

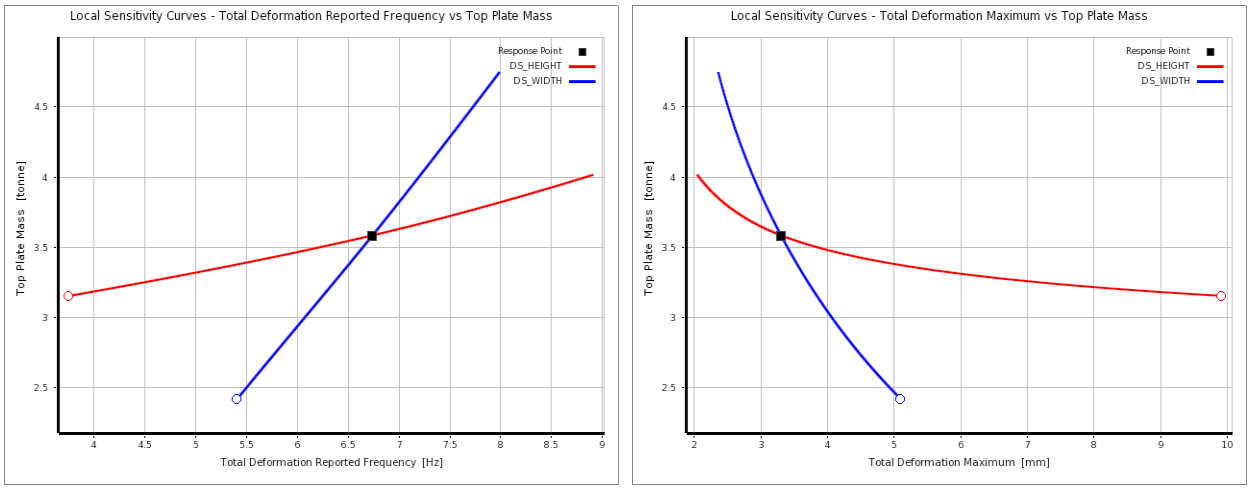

(a) 1st mode frequency with top plate mass (b) Max total deformation with top plate mass

Figure 30. Sensitivity Curves

iv. Optimization

As the dynamic stiffness behavior of top plate was main focus of the optimization study. Three different objective criterions were employed for frequency maximization in order to find an optimum design point.

a) Maximize frequency

b) Frequency greater than target value (as goal)

c) Frequency greater than target value (as hard constraint)

Two different optimization schemes i.e. Screening and MOGA were used for each of these criterions and results obtained for each of these are given below.

a) Maximize Frequency

Setting the objective for frequency as maximization; screening and multi objective genetic algorithm (MOGA) optimization methods were employed to determine the optimum design within the design space. A 3D plot of Pareto fronts obtained as a result of employing MOGA and screening are presented in figure 31. While figures 32 & 33 presents the Pareto fronts obtained for 1st modal frequency with maximum total deformation and top plate mass respectively.

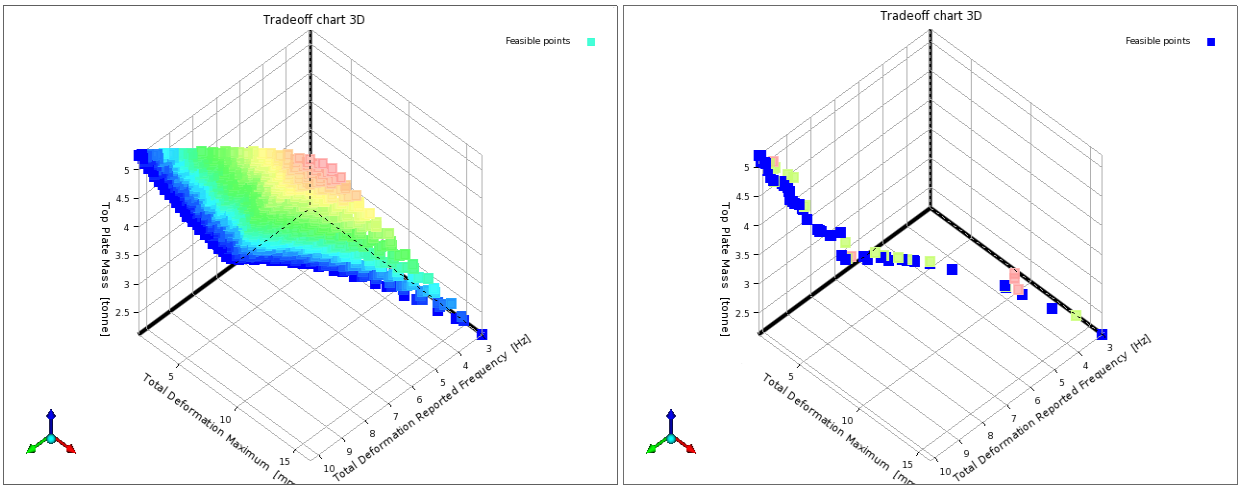

(a) Screening (b) MOGA

Figure 31. 3D Trade off charts for maximize frequency (Hz) objective

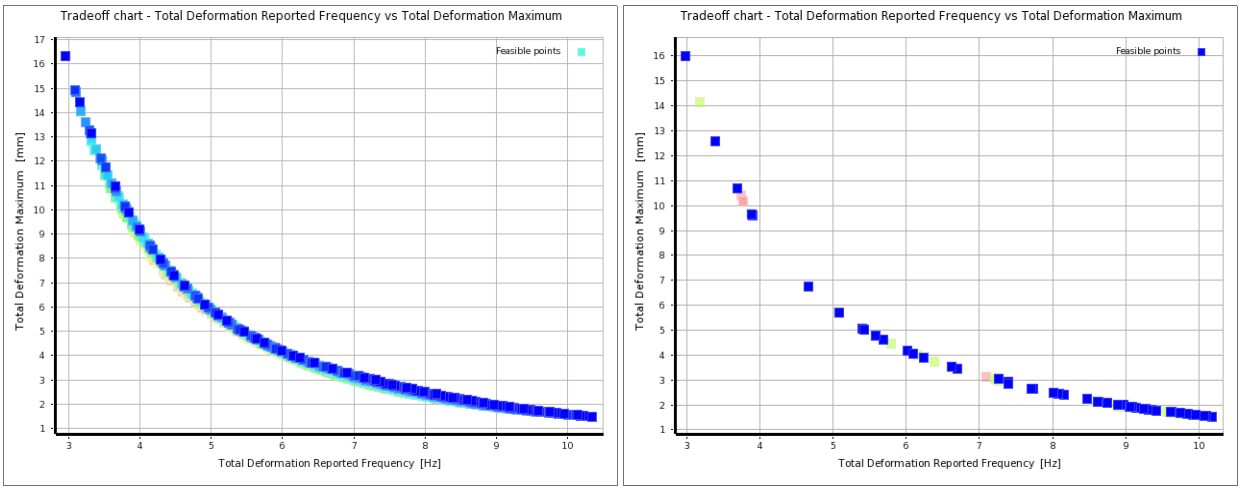

(a) Screening (b) MOGA

Figure 32. 1st mode frequency (Hz) vs. deformation (mm) [maximize freq]

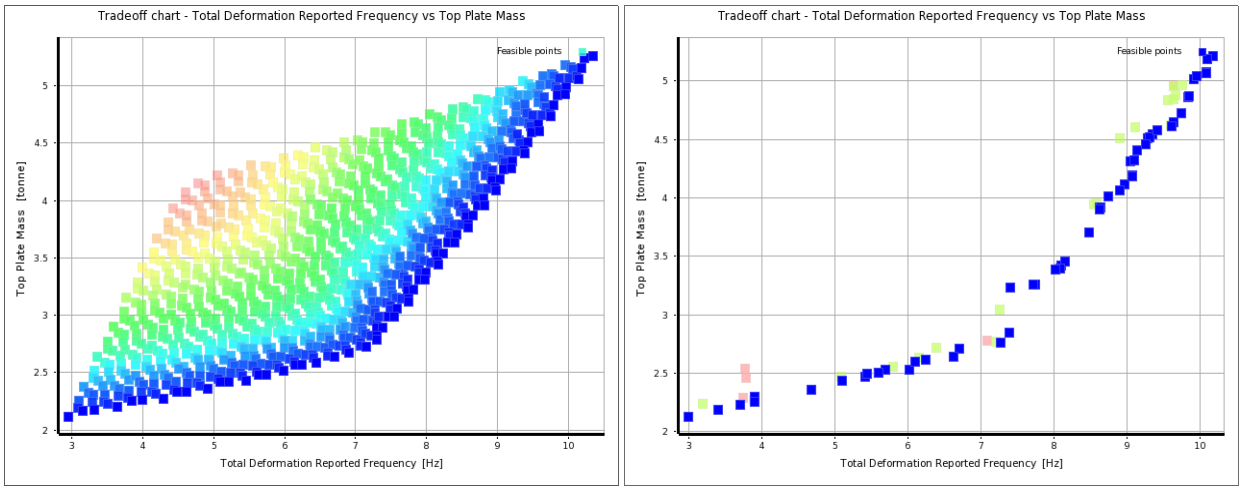

(a) Screening (b) MOGA

Figure 33. 1st mode frequency (Hz) vs. top plate mass (ton) [maximize freq]

The optimum candidate designs obtained as result of employing these two different optimization techniques are presented in Table 13 and 14.

Candidate point	Top plate		Static deformation (mm)	1st modal Frequency (Hz)	Top plate mass (ton)
	Height (mm)	Width (mm)			
A	235	8	3.02	7.31	2.795
B	214	8	3.34	6.87	2.706
C	194	8	3.74	6.42	2.633

Table 13. Optimum candidate points obtained using screening optimization [Max freq]

Candidate point	Top plate		Static deformation (mm)	1st modal Frequency (Hz)	Top plate mass (ton)
	Height (mm)	Width (mm)			
A	235	8	3.05	7.27	2.767
B	205	8	3.55	6.62	2.642
C	185	8	3.91	6.25	2.622

Table 14. Optimum candidate points obtained using MOGA optimization [Max freq]

b) Frequency greater than target value (as goal)

With the operating frequency of top plate as 3Hz and FOS of 3.0 the minimum desired frequency becomes 9Hz. So a value of 9.5 Hz was set as target value in the objective criterion and constraint was set as goal for this optimization. Both screening and multi objective genetic algorithm (MOGA) optimization methods were employed to search the optimum design within the design space. A 3D plot of Pareto fronts obtained as a result of employing MOGA and screening are presented in figure 34. While figures 35 & 36 presents the Pareto fronts obtained for 1st modal frequency with maximum total deformation and top plate mass respectively.

The optimum candidate designs obtained for this optimization scheme using screening and MOGA are presented in Table 15 and 16.

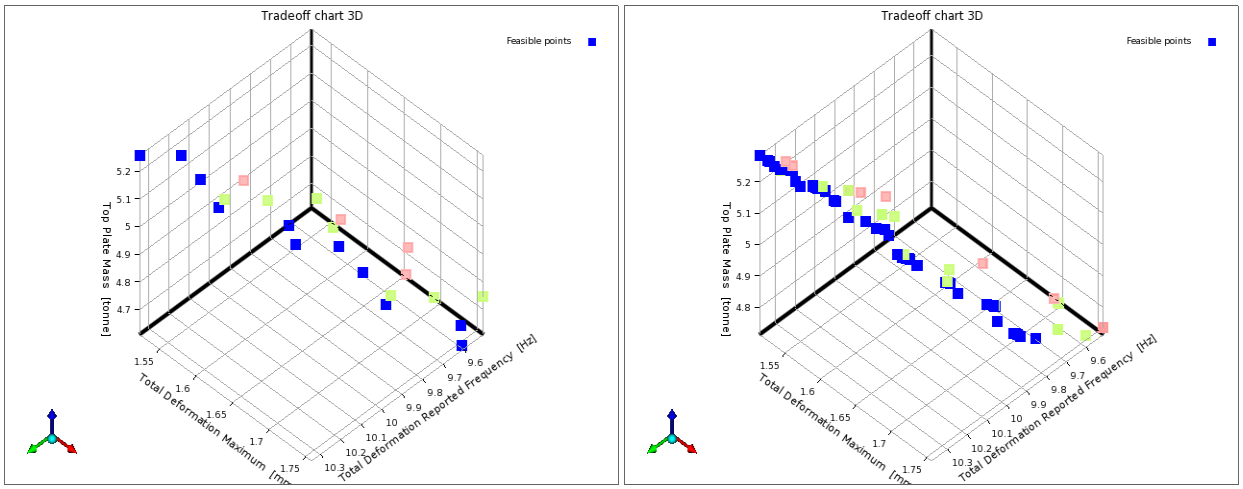

(a) Screening (b) MOGA

Figure 34. 3D Trade off charts for frequency value greater than 9.5Hz objective

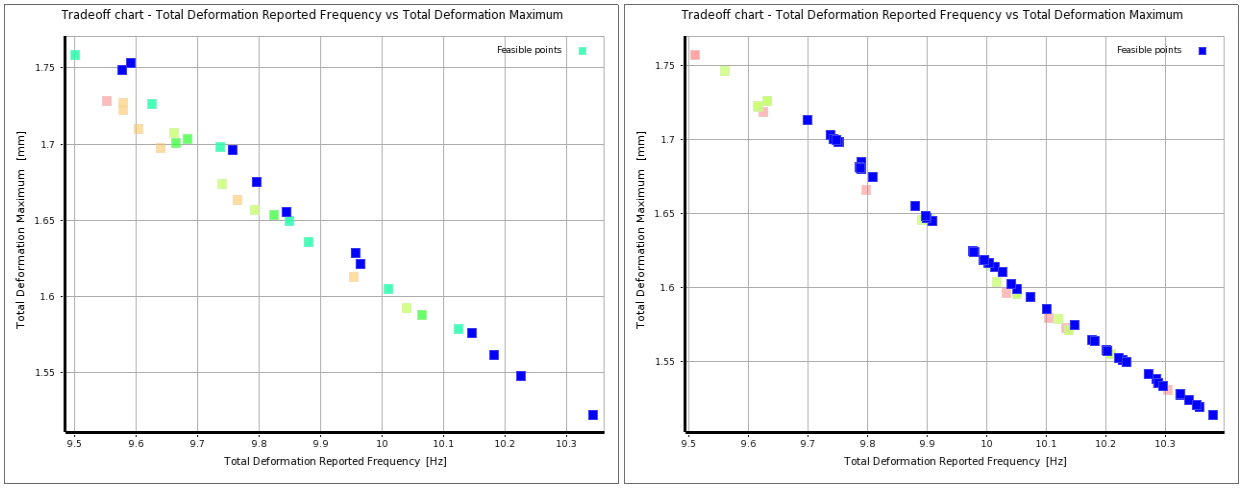

(a) Screening (b) MOGA

Figure 35. 1st mode frequency (Hz) vs. static deformation (mm) [value greater than 9.5Hz]

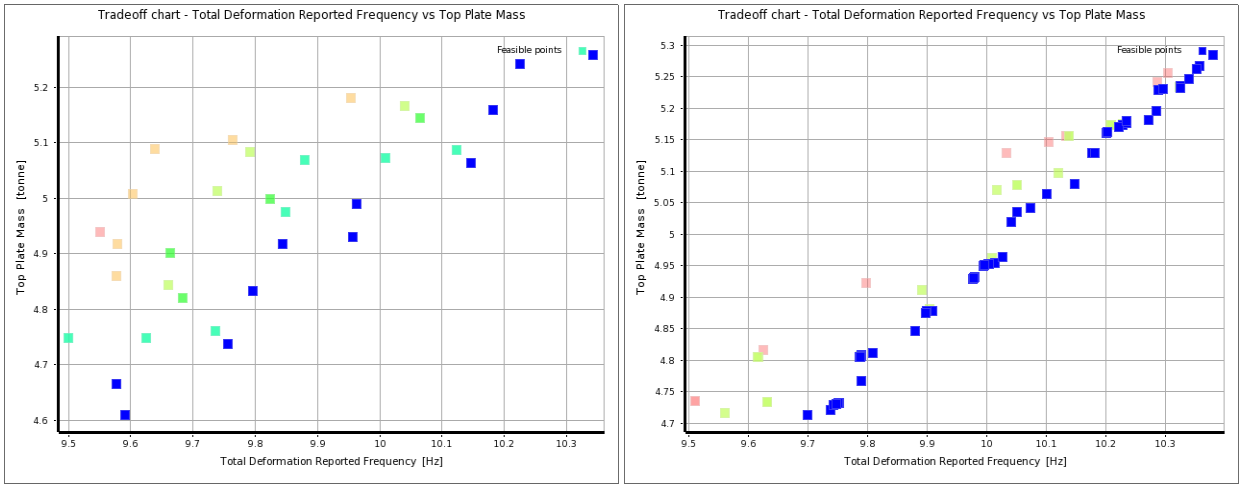

(a) Screening (b) MOGA

Figure 36. 1st mode frequency (Hz) vs. top plate mass (ton) [value greater than 9.5Hz]

Candidate point	Top plate		Static deformation (mm)	1st modal Frequency (Hz)	Top plate mass (ton)
	Height (mm)	Width (mm)			
A	235	8	3.02	7.31	2.795
B	214	8	3.34	6.87	2.706
C	194	8	3.74	6.42	2.633

Table 15. Optimum candidate points obtained using screening [value greater than 9.5Hz (as goal)]

Candidate point	Top plate		Static deformation (mm)	1st modal Frequency (Hz)	Top plate mass (ton)
	Height (mm)	Width (mm)			
A	246	14	1.71	9.70	4.714
B	238	14	1.75	9.56	4.718
C	247	14	1.70	9.74	4.722

Table 16. Optimum candidate points obtained using MOGA [value greater than 9.5Hz (as goal)]

c) Frequency greater than target value (as hard constraint)

Setting the objective criterion for frequency as value greater than target value and constraint handling as hard resulted in the exactly the same Pareto fronts as was obtained in previous section (figure 34-36).The optimum candidate designs search by using Screening and MOGA are given in Table 17 & 18.

Candidate point	Top plate		Static deformation (mm)	1st modal Frequency (Hz)	Top plate mass (ton)
	Height (mm)	Width (mm)			
A	246	14	1.75	9.59	4.611
B	242	14	1.75	9.58	4.665
C	240	14	1.73	9.63	4.749

Table 17. Optimum candidate points obtained using screening [value greater than 9.5Hz]

Candidate point	Top plate		Static deformation (mm)	1st modal Frequency (Hz)	Top plate mass (ton)
	Height (mm)	Width (mm)			
A	246	14	1.71	9.70	4.714
B	238	14	1.75	9.56	4.718
C	247	14	1.70	9.74	4.722

Table 18. Optimum candidate points obtained using MOGA [value greater than 9.5Hz]

As ours objective was to optimize the dynamic response of top plate. So the candidate having the maximum frequency i.e. designs C, obtained using MOGA, for frequency greater than target value (as hard constraint), was selected as optimized design. Thus the optimum design of top plate based on size optimization has following characteristics (Table 19).

Height (mm)	247
Rib Thickness (mm)	14.0
Top plate mass (ton)	4.722
Static Deformation (mm)	1.70
1st mode frequency (Hz)	9.74

Table 19. Salient features of optimum top plate design obtained after size optimization

2. Shape optimization

After finalizing the top plate height and rib thickness based on size optimization study. Shape of the optimized structure obtained was optimized in order to reduce its weight guaranteeing the stiffness characteristics desired set for final design. For this purpose a step plate design (figure 37) is used in which

a) Height of top plate is increased at centre section where a payload is to be mounted
b) Whereas the height at outer section is decreased in order to achieve the purpose of mass reduction without any significant loss in static and dynamic stiffness

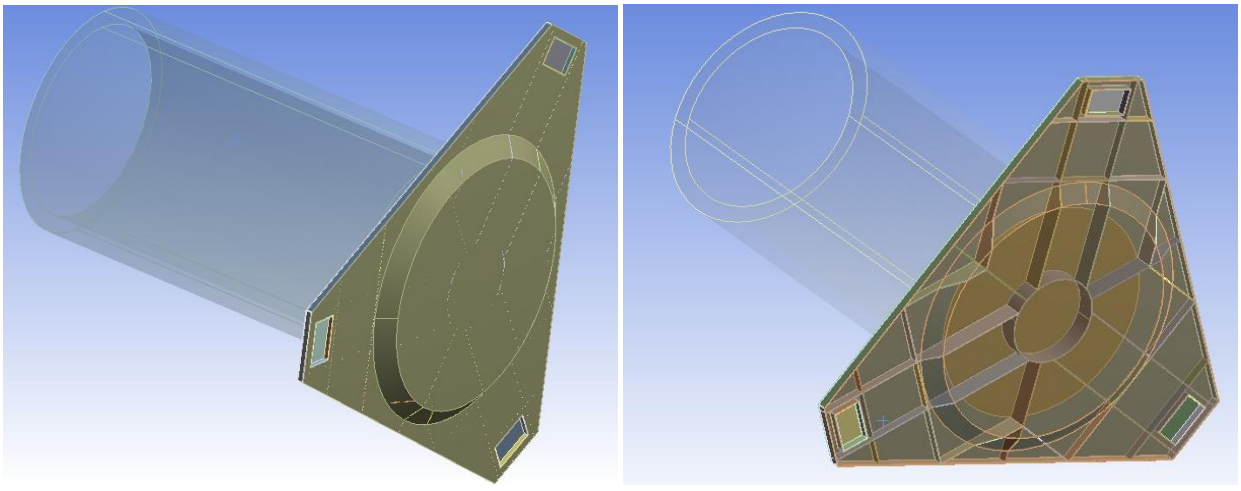

(a) Outer structure (b) Rib structure

Figure 37. Preview of top plate design used for shape optimization

Thus the three design variables for carrying out shape optimization are top plate height at centre (DS_total height), top plate height at outer section (DS_outside height)and rib thickness (DS_width). Two different cases were run for this purpose.

Case 1

All the three variables were varied in order to have an optimized design in terms of mass producing the desired performance. DOE and MOGA optimization is used. The optimization problem is formulated as follows

Objectives:

Minimize Top plate mass (ton)

Constraints:

Frequency ≥ 9.0 Hz
Static total deformation ≤ 2 mm
12 ≤ Rib thickness (mm) ≤ 18
60 ≤ Rib height at outer section (mm) ≤ 180
200 ≤ Rib height at center section (mm) ≤ 230

i. DOE Matrix

DOE matrix used for input parameters and results of mass, static total deformation and 1st mode frequency are shown in figure 38.

Table of Schematic D2: Design of Experiments (Central Composite Design : Face-Centered : Enhanced)

	A	B	C	D	E	G	I
1	Name	P6 - DS_WIDTH	P7 - DS_OUTSIDE_HEIGHT	P10 - DS_TOTAL_HEIGHT	P1 - Total Deformation Reported Frequency (Hz)	P4 - Total Deformation Maximum (mm)	P9 - Top Plate Mass (tonne)
2	1	15	116	215	7.4732	2.3239	4.5368
3	2	12	116	215	6.4272	3.0265	3.6312
4	3	13.5	116	215	6.9672	2.6169	4.0841
5	4	18	116	215	8.4698	1.8752	5.4416
6	5	16.5	116	215	8.004	2.0692	4.9893
7	6	15	56	215	4.5747	7.3976	4.2683
8	7	15	86	215	6.2348	3.6543	4.4011
9	8	15	176	215	9.5086	1.2587	4.8193
10	9	15	146	215	8.5502	1.6579	4.676
11	10	15	116	200	7.4484	2.3412	4.5036
12	11	15	116	207.5	7.4602	2.327	4.5201
13	12	15	116	230	7.5104	2.3093	4.5709
14	13	15	116	222.5	7.5098	2.3194	4.5537
15	14	12	56	200	4.0601	9.0168	3.3869
16	15	13.5	86	207.5	5.7592	4.1787	3.946
17	16	18	56	200	5.5291	5.1137	5.0766
18	17	16.5	86	207.5	6.6635	3.2255	4.8209
19	18	12	176	200	8.1604	1.6225	3.8344
20	19	13.5	146	207.5	7.9307	1.8809	4.1953
21	20	18	176	200	10.616	1.0424	5.7451
22	21	16.5	146	207.5	9.0916	1.4913	5.125
23	22	12	56	230	3.8937	9.8773	3.4454
24	23	13.5	86	222.5	5.7752	4.2064	3.9778
25	24	18	56	230	5.3119	5.5932	5.164
26	25	16.5	86	222.5	6.6581	3.2527	4.8596
27	26	12	176	230	8.2242	1.6123	3.8818
28	27	13.5	146	222.5	7.9568	1.871	4.2239
29	28	18	176	230	10.741	1.0228	5.8159
30	29	16.5	146	222.5	9.1405	1.4809	5.1598

Figure 38. DOE matrix used for shape optimization [Case 1]

ii. Response Surface

The 3D response curves of 1st modal frequency, static deformation and top plate mass against the design variables are shown in figures 39-41. Figures 42-44 show the response of all these three objectives with variation in height at centre, outside height and thickness of ribs individually. Response curves are clearly showing that for a fixed value of rib thickness and outside height; apart from adding to total mass variation in top plate height at centre plays no role in increasing the stiffness characteristics of top plate. Thus total height at centre is redundant variable while carrying out the optimization study.

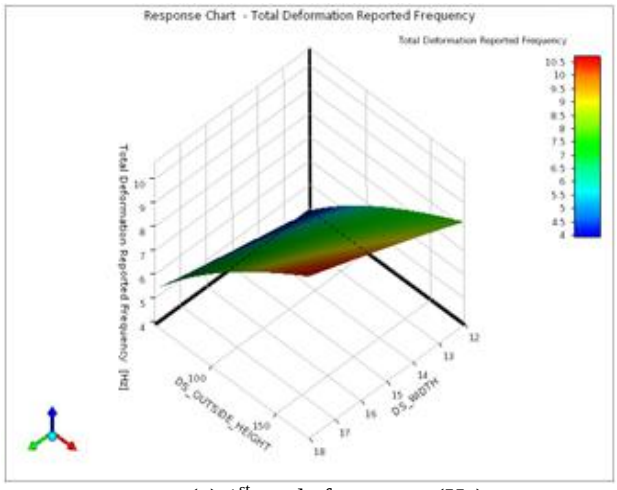

(a) 1st mode frequency (Hz)

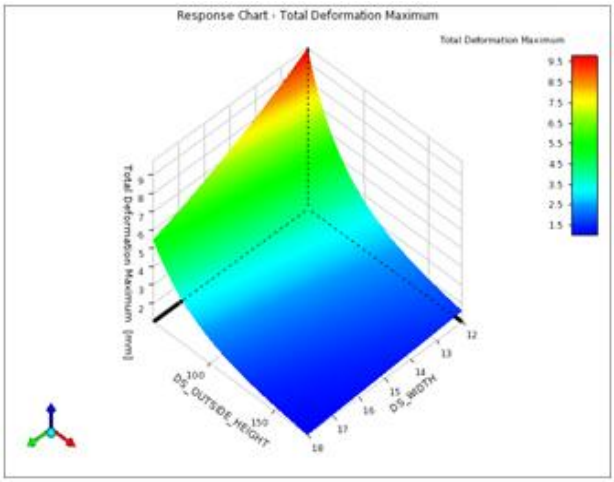

(b) Static total deformation (mm)

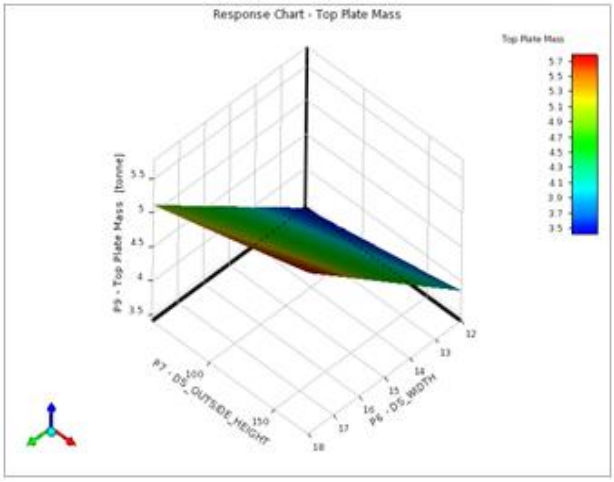

(c) Top plate mass (ton)

Figure 39. 3D response surfaces against DS_outside_height & DS_width parameters

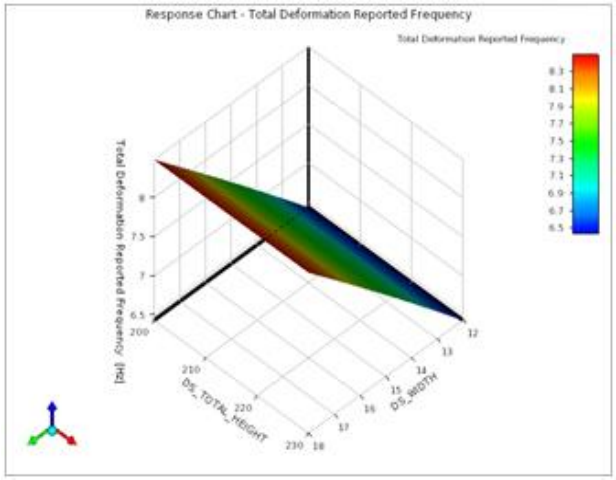

(a) 1st mode frequency (Hz)

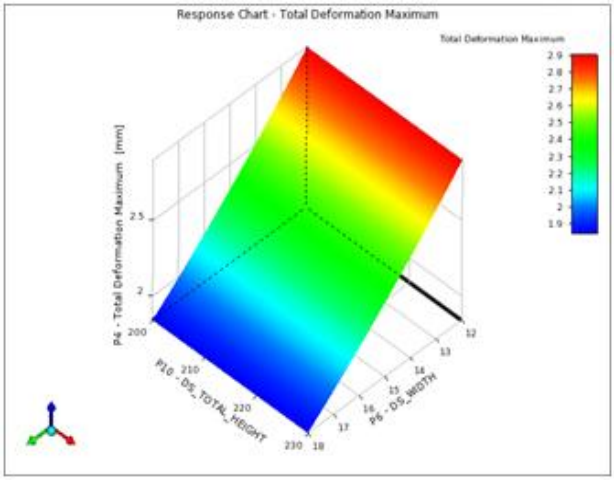

(b) Static total deformation (mm)

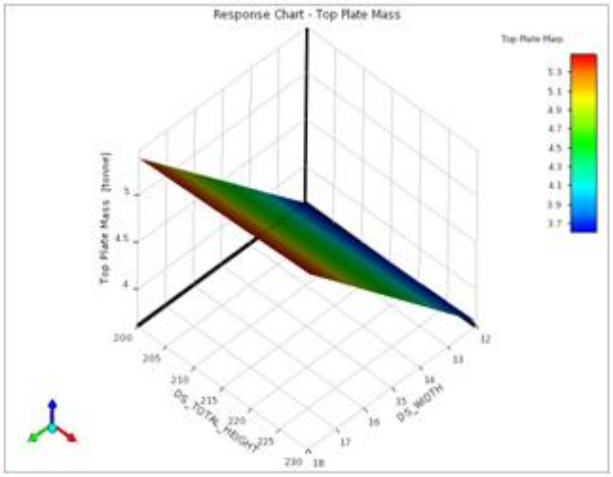

(c) Top plate mass (ton)

Figure 40. 3D response surfaces against DS_total_height & DS_width parameters

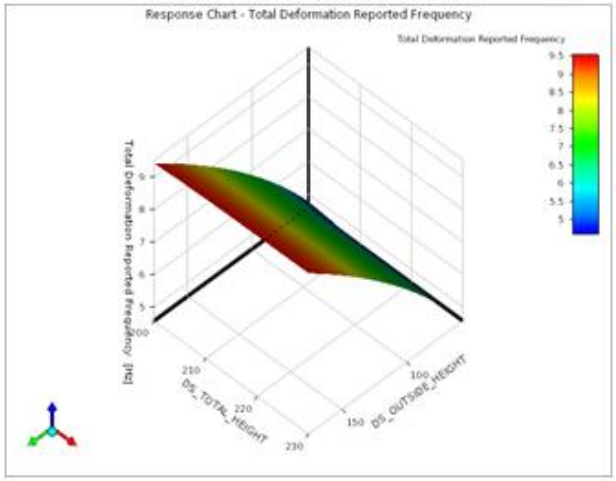

(a) 1st mode frequency (Hz)

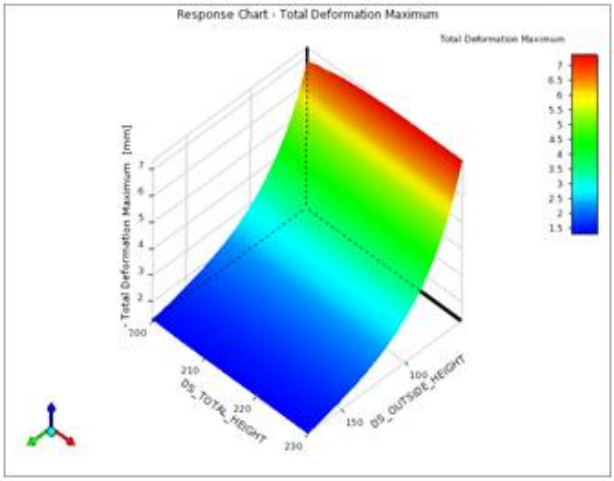

(b) Static total deformation (mm)

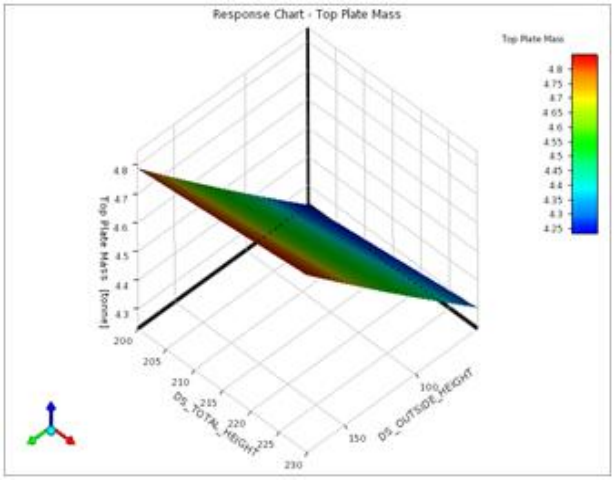

(c) Top plate mass (ton)

Figure 41. 3D response surfaces against DS_outside_height & DS_total_height parameters

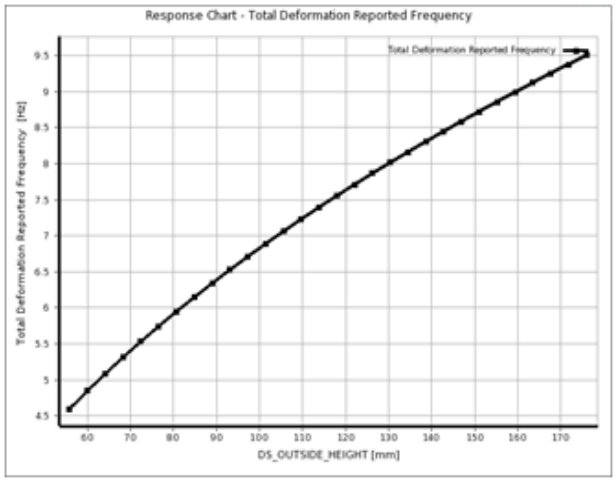

(a) DS_outside_height parameter

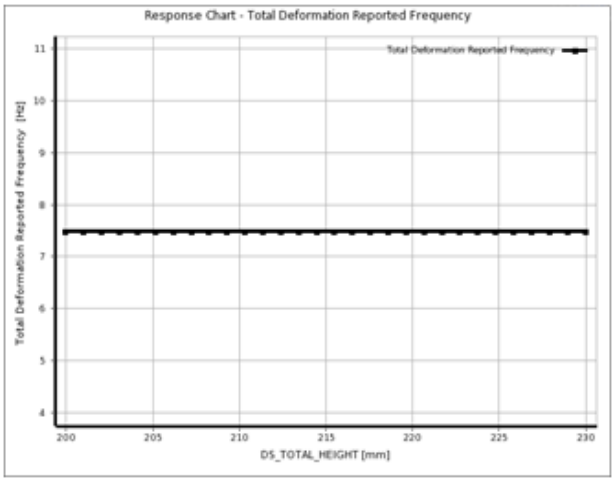

(b) DS_total_height parameter

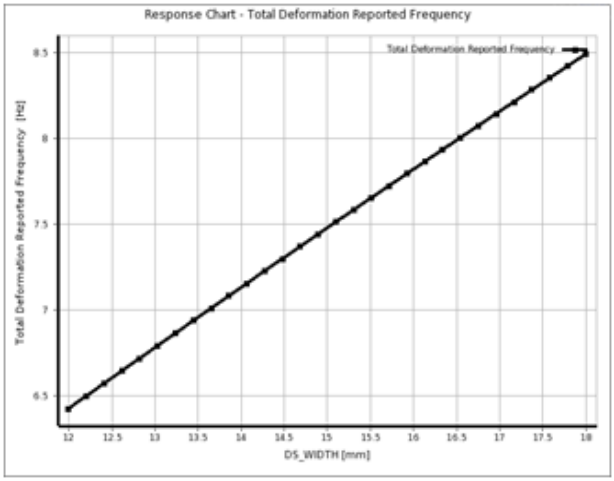

(c) DS_width Parameter

Figure 42. 1st mode Frequency (Hz) variation

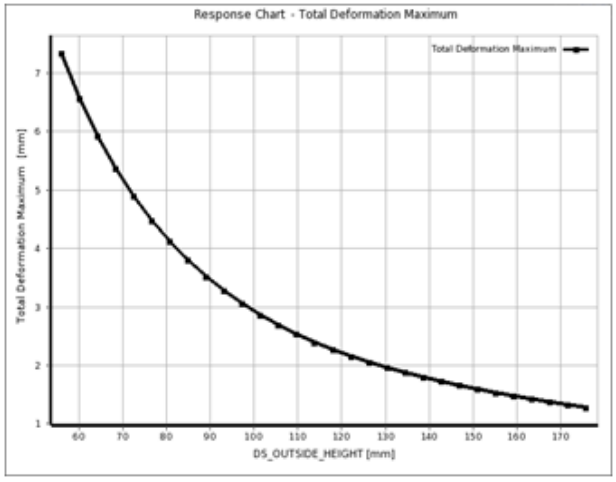

(a) DS_outside_height parameter

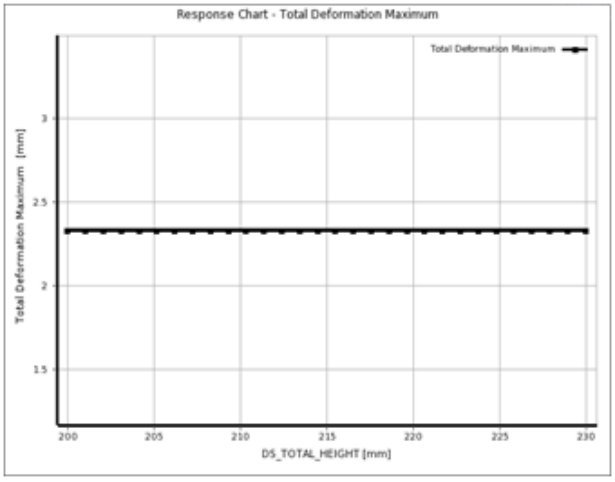

(b) DS_total_height parameter

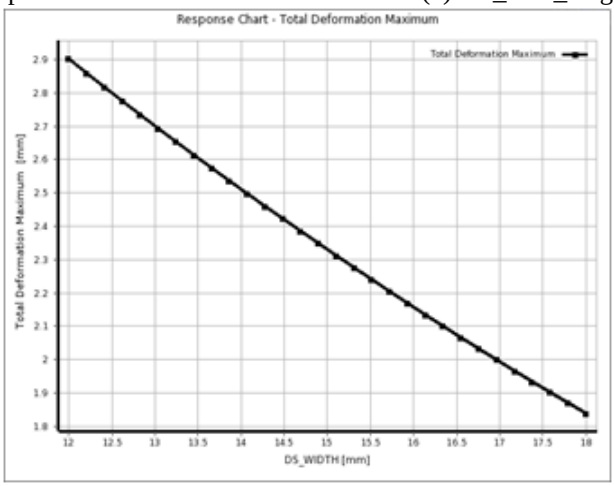

(c) DS_width Parameter

Figure 43. Static total deformation (mm) variation

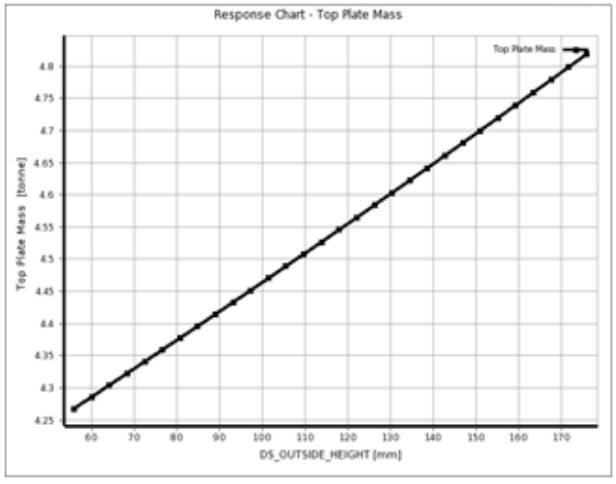

(a) DS_outside_height parameter

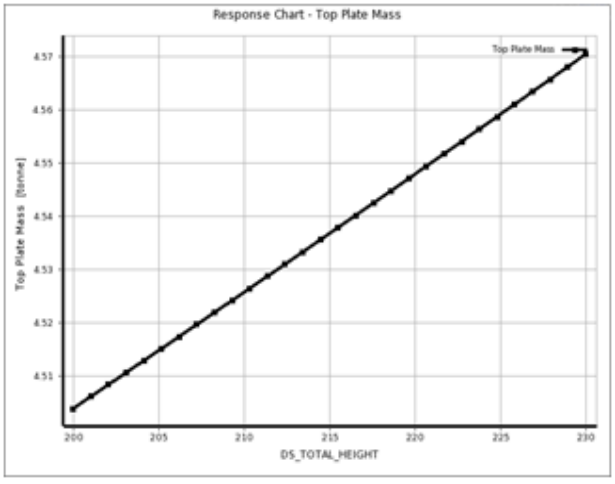

(b) DS_total_height parameter

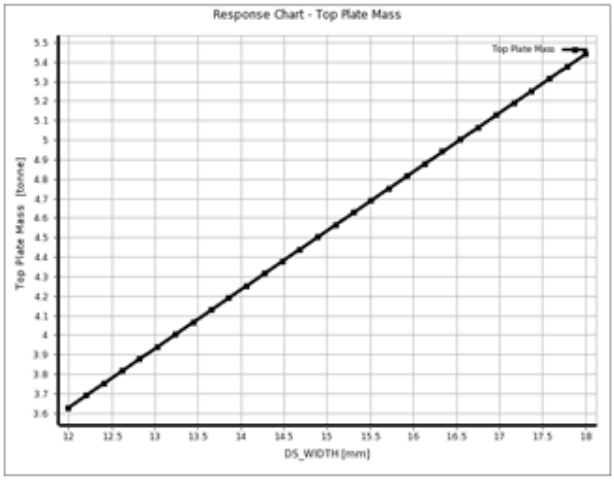

(c) DS_width Parameter

Figure 44. Top plate mass (ton) variation

iii. Sensitivity Analysis

The bar graph of sensitivities of 1st modal frequency, static total deformation and top plate mass are shown in figure 45. Sensitivity analysis also predicted the same results i.e. total height parameter is redundant and is not required during the weight optimization study.

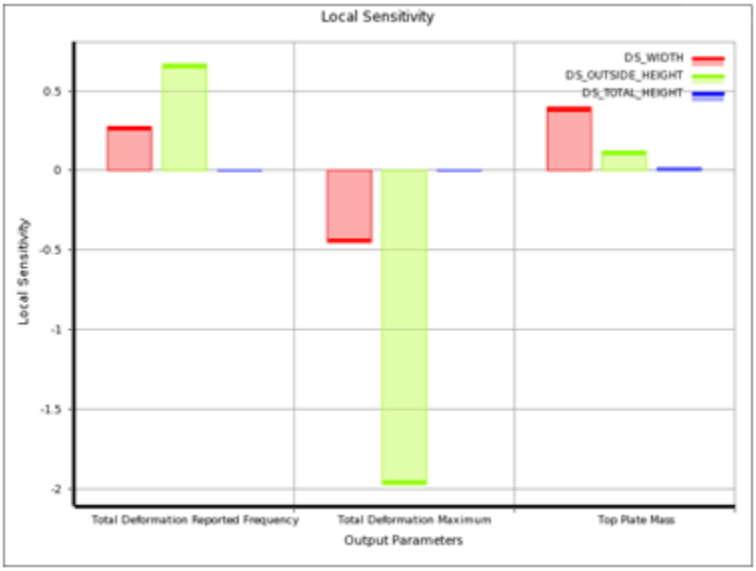

Figure 45. Local sensitivity of output parameters [Shape optimization Case 1]

iv. Optimization

MOGA optimization technique was employed to determine the optimum design among the search space. 1st mode frequency was constraint to value greater than 9 Hz in order to meet the objective set for dynamic stiffness. As the primary purpose of this optimization was to reduce the

mass of top plate so objective criterion for top plate mass was set as target value less than 4.5 ton (hard constraint). Optimum candidate points obtained are given in Table 20. Optimization study for this case effectively yielded one optimum point. The value obtained for rib thickness of the structure is same as obtained through size optimization study.

Candidate point	Top plate			Static deformation (mm)	1st modal Frequency (Hz)	Top plate mass (ton)
	Height at centre (mm)	Outside Height (mm)	Rib Thickness (mm)			
A	252	203	14	1.40	9.06	4.498
B	253	203	14	1.40	9.06	4.499
C	253	203	14	1.40	9.06	4.500

Table 20. Optimum candidate points for shape optimization using MOGA [Case 1]

Case 2

Upon reviewing the results of case 1 it was found that height of top plate at centre is redundant variable for shape optimization study and rib thickness yielded the same results as size optimization. A second case was run in which the top plate design obtained through size optimization was further optimized for weight. In this case the height of top plate and rib thickness were kept the same as obtained in size optimization study i.e. 247 mm & 14 mm respectively. The shape of the top plate was varied by removing the material from the outer sections. The optimum height of ribs for the outer section is determined using DOE and MOGA optimization. The optimization problem formulated is shown below.

Objectives:

Minimize Top plate mass (ton)

Constraints:

Frequency $\geq$ 9.0 Hz
Static total deformation $\leq$ 2mm
60 $\leq$ Rib height at outer section (mm) $\leq$ 180

i. DOE Matrix

DOE matrix used for input parameters and results of mass, static total deformation and 1st mode frequency are shown in figure 46.

	A	B	C	D	F
1	Name	P7 - DS_OUTSIDE_HEIGHT	P1 - Total Deformation Reported Frequency (Hz)	P4 - Total Deformation Maximum (mm)	P9 - Top Plate Mass (tonne)
2	1	116	7.4939	2.3202	4.5458
3	2	116	6.4539	2.9907	3.6384
4	3	116	6.9525	2.6214	4.0922
5	4	116	8.4965	1.8676	5.4524
6	5	116	7.9865	2.0705	4.9992
7	6	56	4.5721	7.4501	4.278
8	7	86	6.2332	3.6625	4.4105
9	8	176	9.552	1.2592	4.8272
10	9	146	8.5632	1.6474	4.6845
11	10	56	3.821	10.304	3.4237
12	11	86	5.7751	4.1929	3.9703
13	12	56	5.2822	5.6397	5.1316
14	13	86	6.6677	3.246	4.8505
15	14	176	8.1793	1.624	3.864
16	15	146	7.9728	1.8646	4.2172
17	16	176	10.666	1.0322	5.7893
18	17	146	9.1391	1.4822	5.1516

Figure 46. DOE matrix used for shape optimization [Case 2]

ii. Response Surface

The response curves obtained as result of DOE are shown in figure 47. The curves show that the 1st modal frequency and top plate mass vary almost linearly with variation in outside height.

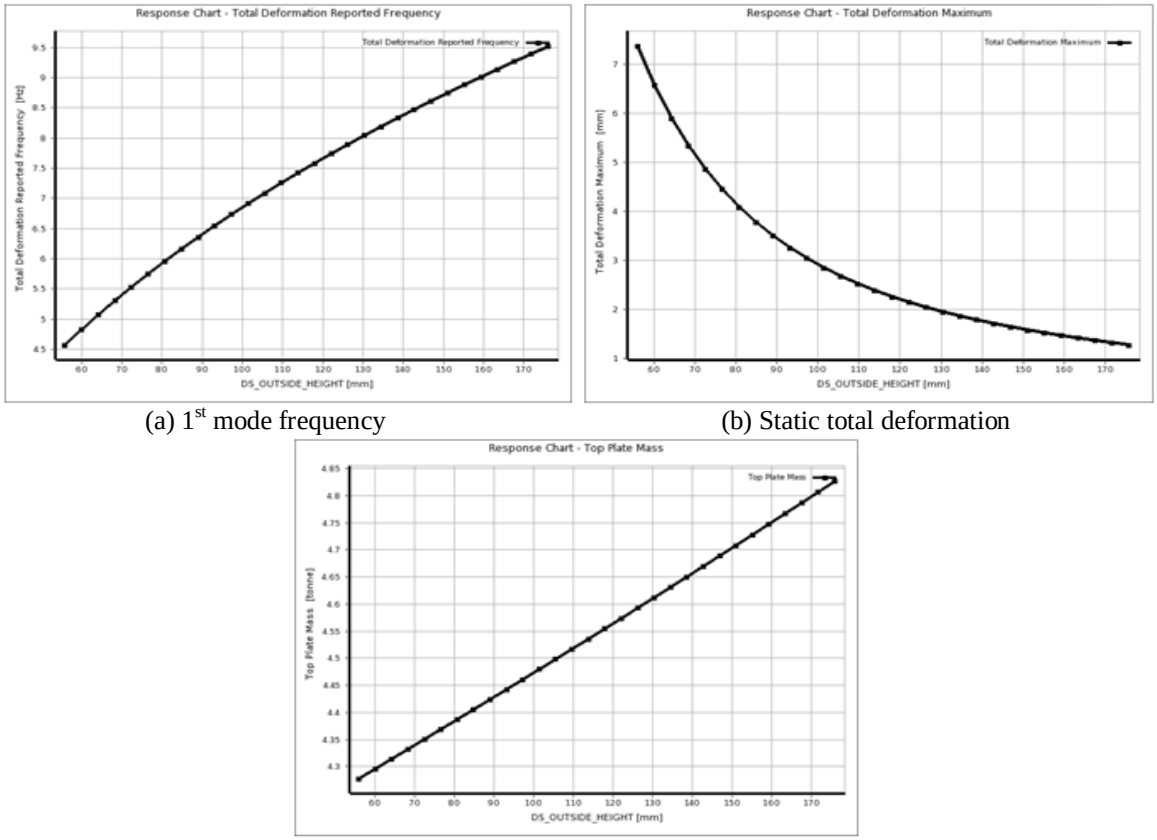

(a) 1st mode frequency (b) Static total deformation

(c) Top plate mass

Figure 47. Response curves for shape optimization study [Case 2]

iii. Optimization

MOGA optimization technique was employed to determine the optimum design among the search space. 1st mode frequency was constraint to value greater than 9 Hz in order to have a design meeting the required dynamic stiffness and objective criterion for top plate mass was set as target value less than 4.5 ton (hard constraint). The optimum candidate designs obtained are presented in Table 21. Candidate B was selected as final optimized design of top plate.

Candidate point	Top plate		Static deformation (mm)	1st modal Frequency (Hz)	Top plate mass (ton)
	Outside Height (mm)	Width (mm)			
A	201	14	1.42	9.00	4.482
B	201	14	1.42	8.99	4.480
C	200	14	1.43	8.94	4.457

Table 21. Optimum candidate points for shape optimization using MOGA [Case 2]

Once the optimum design for top plate have been selected a comparative analysis was done in order to quantify the amount of weight loss that have been achieved through the shape optimization study. For this purpose weight of top plate design obtained after size optimization have been compared with the final optimized design. A weight reduction of 5.12 % has been achieved by employing the shape optimization (Table 22).

Original weight (ton)	Optimized weight (ton)	Difference (ton)	Reduction (%)
4.722	4.480	0.242	5.12

Table 22. Weight Reduction achieved through shape optimization

4. FEM Results

The parametric model of this final optimum design was developed according to specifications given in Table 23 and stiffness behavior was analyzed using ANSYS workbench.

Top plate mass (ton)	4.480
Top plate height at centre (mm)	247
Height of outer section (mm)	201
Upper & Lower plate thickness (mm)	14.0
Rib thickness (mm)	14.0
Circular rib diameter (mm)	1000
Joint attachment geometry (mm^3)	500 x 300 x 160

Table 23. Specifications of final optimized design

The static stiffness results obtained are tabulated in Table 24 and deformation contours in figure. 48. Table 25 presents the dynamic stiffness results while mode shapes for first three frequencies are shown in figure 49-51. The static total deformation is less than 2mm and 1st modal frequency is 9 Hz. Thus design is meeting the desired stiffness criterion set initially for satisfactory performance therefore the design was carried forward for prototype development.

Static total deformation (mm)	1.3935

Table 24. FEM results for Static stiffness of optimized design

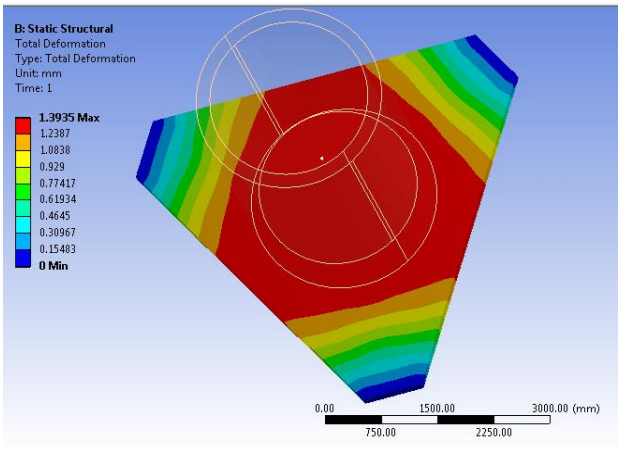

Figure 48. Static deformation contours (Optimized design)

Mode	Frequency (Hz)
1st	**8.9931**
2nd	9.0153
3rd	13.501
4th	69.878
5th	70.408
6th	113.3

Table 25. FEM results for dynamic stiffness of optimized design

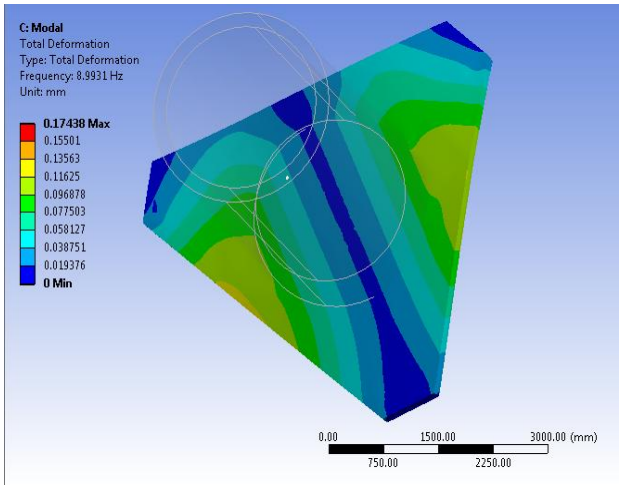

Figure 49. 1st mode shape contours (Optimized design)

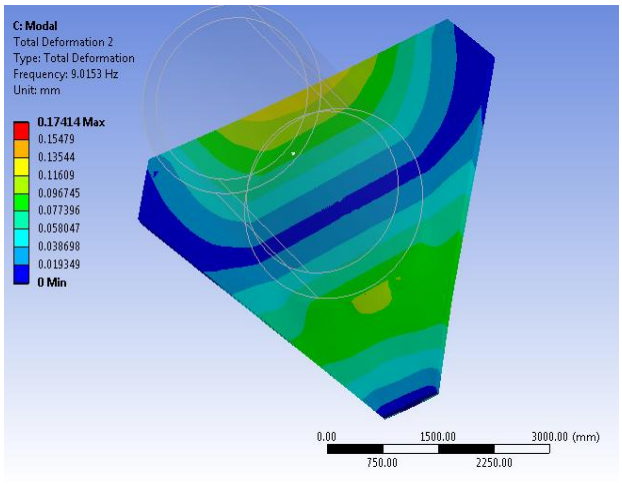

Figure 50. 2nd mode shape contours (Optimized design)

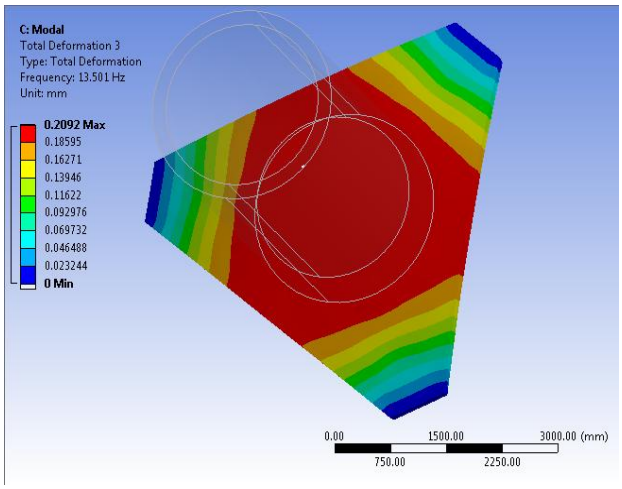

Figure 51. 3rd mode shape contours (Optimized design)

5. Experimental testing

A prototype of final optimized structure was developed and experimental testing was carried out in order to determine the actual stiffness characteristics. The test conditions and procedure was same as adopted for testing of detailed model. The results obtained are shown in Table 26.

Top Plate Mass (ton)				4.5		
	P0	**P1**	**P2**	**P3**	**P4**	**Avg. Value**
Static (mm)	1.3	1.1	1.4	1.4	1.5	1.34
1st Modal (Hz)	8.9	8.9	9.5	9.9	8.8	9.20

Table 26. Experimental values for top plate (Optimized design)

6. Evaluation of results

The results obtained from FEM modeling were evaluated by comparing them with the experimental results in the form of percentage relative error and are tabulated in Table 27. There is a good agreement between results obtained through FEM models and physical experiments. The maximum relative error obtained is 9.1% and 6.9% for 1st mode frequency and static deformation respectively. While average error for fundamental frequency is 3.8% and 8.3 for static total deformation. These small errors again emphasize that line contact boundary condition for joint is to be applied if realistic prediction of stiffness characteristics is to be achieved.

	P0	P1	P2	P3	P4	Avg. Value
Static (%)	6.9	26.3	0.7	0.7	7.3	8.4
1st Modal (%)	1.0	1.0	5.4	9.1	2.2	3.8

Table 27. Relative error between experimental & FEA results (Optimized design)

FUTURE SCOPE

The subject thesis was an attempt towards the accurate prediction of stiffness behavior of 6-DOF top plate. The analysis work is done considering only one pose of platform and only contact stiffness of associated joints is considered. Therefore, there is a lot of room for further research in the concept at hand. The future work can be related to a mix of procedures given below:

a) Finding a global stiffness response by carrying out an analysis for various poses of platform within the workspace to determine its behavior throughout the whole workspace.

b) Finding the effect of various other complexities that can arise in joints such as Joint clearance, as it also plays a critical role in overall stiffness. An analysis considering both the different contact types and clearance can be carried out to have even more realistic prediction of platform's behavior.

CONCLUSION

In this thesis an accurate simulation driven stiffness modeling methodology has been proposed for top plate of special application of 6-DOF platforms i.e. subjected to heavy loads. Both static and dynamic stiffness characteristics, in terms of total deformation and frequency, have been analyzed for simplified model and detailed model. The FEM results have been verified with those obtained through experimental testing.

The thesis started with introduction of parallel manipulators and their applications in the various fields wherein a special emphasize was laid on 6-DOF manipulators as it was topic of current research. Moreover various advantages and challenges associated with these manipulators are also highlighted. In literature review importance of stiffness modeling of parallel manipulators has been discussed in detail. Various techniques that have developed over the years for modeling and analyzing the stiffness characteristics are discussed. Joints, different complexities associated with the joints and issues pertaining to modeling these complexities have also been presented. The optimization work that has been done in regard to parallel platforms and various aspects/components that are covered in optimization studies are highlighted.

Next in, a detailed and comprehensive step by step methodology adopted for carrying out the work has been explained. The effect of considering different joint boundary conditions on stiffness of top plate has been analyzed in the next section. At first a simplified FEM model has been developed wherein the joint complexities were ignored and stiffness behavior has been analyzed. Then a detailed modeling incorporating various types of joint contacts has been done to analyze the static and dynamic stiffness response. The results obtained through simplified and detailed modeling are compared and analyzed, which depicts that by taking into account the contact stiffness of joints the relative error between FEM and experimental results has reduced from 61.5 to 13.7 % and the average error from 52.1 to 8.7% for 1^{st} mode frequency. This shows the contact stiffness of joints has a significant effect on accuracy of the model.

Thus results obtained through this work depict that the correct application of boundary conditions for heavily loaded 6-DOF platforms is highly essential for realistic prediction of static and dynamic response to applied load.

At the end GA based size and shape optimization techniques have been used to reach a design meeting the required stiffness characteristics. A weight reduction of 5.1% has been achieved through shape optimization.

Considering the scarcity of available references for employing correct analysis technique for this particular application area. This work will not only serve as a guideline for future work but also provide the correct methodology for simulation driven design of platform's top plate thus reducing the dependency on experimental work and amount of testing required.

Last future work for the research was discussed by giving various options through which the current study can be made more fruitful and vast in terms of both the deliverables and optimum operative performance.

REFERENCES

Stewart, D., 1965, "A platform with six degrees of freedom", in Proceedings of the Institution of Mechanic al Engineers, Vol. 180, pp. 371-378.

Ilian Alexandrov Bonev, 1998, "Analysis and design of 6-DOF 6-PRRS parallel manipulators", Master Thesis, Kwangju Institute of Science and Technology, Korea.

McCallion, H., and Pham, D. T., 1979, "The Analyses of a Six Degrees of Freedom Work Station for Mechanized Assembly", 5th World Congress on Theory of Machines and Mechanisms, pp. 611-616, Montréal.

Grace, K. W., 1995, "Kinematic Design of an Ophthalmic Surgery Robot and Feature Extracting Bilateral Manipulation", Doctorate Dissertation, Northwestern University, Evanston (IL).

Lazarevic, G., 1997, "Feasibility of a Stewart Platform with Fixed Actuators as a Platform for CABG Surgery Device", Master Thesis, Columbia University, New York (NY).

Anderson, E. H., Cash, M. F., Hall, J. L., and Pettit, G. W., 2004 , "Hexapods for precision motion and vibration control," American Society for Precision Engineering, Control of precision systems, April 2004.

Hall, J. L., Pettit, G. W., Lindler, J. E., Anderson, E. H., Flint, E. M., 2003, "Compact lightweight six-axis point-and-hold positioning system," Smart structures and materials 2003: Industrial and commercial applications of smart structures technologies, p 287-300, v 5054.

Memet Unsal, 2006, "Semi-active vibration control of a parallel platform mechanism using magnetorheological damping", Doctorate Dissertation, University of Florida, Florida.

Aftab Ahmad, Kjell Andersson, Ulf Sellgren, Suleman Khan, 2012, "A stiffness modeling methodology for simulation-driven design of haptic devices". Engineering with Computers, Springer Verlog London, January 2014, Volume 30, Issue 1, pp 125-141.

Dan Zhang, 2000, "Kinetostatic analysis and optimization of parallel and hybrid architectures for machine tools"", Doctorate Dissertation, Laval University , Quebec, Canada.

Liu, M. J., Li, C. X., and Li, C. N., 2000, "Dynamics Analysis of the Gough-Stewart Platform Manipulator," IEEE Transactions on Robotics and Automation, 16(1), pp. 94-98.

Mahmoodi, A., Menhaj, M. B., and Sabzehparvar, M., 2009, "An Efficient Method for Solution of Inverse Dynamics of Stewart Platform," Aircraft Engineering and Aerospace Technology, 81 (5), pp. 398-406.

Vakil, M., Pendar, H., and Zohoor, H., 2008, "Closed-Form Dynamic Equations of the General Stewart Platform through the Newton-Euler Approach" and "A Newton-Euler Formulation for the Inverse Dynamics of the Stewart Platform Manipulator"," Mechanism and Machine Theory, 43(10), pp. 1349-1351.

X. Kong and C.M. Gosselin, 2001, "Generation and forward displacement analysis of two new classes of analytic 6-SPS parallel manipulators", Journal of Robotic Systems 18,pp. 295-304.

N.D. Perreira, 1999, "Motions, efforts and actuations in constrained dynamic systems: a multilink closed chain example", Journal of Robotic Systems 16,pp. 363-385.

J. Zhiming and L. Zhenqun, 1999, "Identification of placement parameters for modular platform manipulators", Journal of Robotic Systems 16, pp. 227-236.

F. Hao, J.M. McCarthy, 1998, "Conditions for line-based singularities in spatial platform manipulators", Journal of Robotic Systems 15, pp. 43-55.

J.J. Hall and R.L. Williams II, 2000, "Inertial measurement unit calibration platform", Journal of Robotic Systems, 17, pp. 623-632.

R.G. Selfridge and G.K. Matthew, 2000, "Forward Analysis of Some Special Stewart Platforms", Journal of Robotic Systems, 17, pp. 517-526.

J. Park, B. Kim, J. Song, H. Kim, 2008 "Safe link mechanism based on nonlinear stiffness for collision safety", Mechanism and Machine Theory 43(10), pp 1332-1348.

J. Angeles, F. Park, 2008 "Performance Evaluation and Design Criteria", in: B. Siciliano, O. Khatib, (Eds.), Handbook of robotics, Springer, Berlin, pp. 229-243.

A. De Luca, W. Book, 2008, "Robots with Flexible Elements", in: B. Siciliano, O. Khatib, (Eds.), Handbook of robotics, Springer, Berlin, pp. 287-319.

Sh. Y. Nof, (Ed.), 1999, "Handbook of industrial robotics", John Wiley, New York.

M A. Meggiolaro, S Dubowsky, C Mavroidis, 2005, "Geometric and elastic error calibration of a high accuracy patient positioning system", Mechanism and Machine Theory 40, pp 415 – 427.

S. Timoshenko, J. N. Goodier, 1970, "Theory of elasticity", 3rd Ed., McGraw-Hill, New York.

K. D. Hjelmstad, 1997, "Fundamentals of structural mechanics", Prentice-Hall, New York.

J. Duffy, 1996, "Statics and kinematics with applications to robotics", Cambridge University Press, New York.

D. Deblaise, X. Hernot, P.Maurine, 2006 "A systematic analytical method for PKM stiffness matrix calculation", In: Proceedings of the IEEE International Conference on Robotics and Automation (ICRA), Orlando, Florida, pp. 4213-4219.

H. C. Martin, 1966,"Introduction to matrix methods of structural analysis", McGraw-Hill Education.

Y.W. Li, J.S. Wang, L.P. Wang, 2002, "Stiffness analysis of a Stewart platform-based parallel kinematic machine", In: Proceedings of IEEE International Conference on Robotics and Automation (ICRA), Washington, US, pp. 3672–3677.

K. Nagai, Zh. Liu, 2008,"A Systematic Approach to Stiffness Analysis of Parallel Mechanisms", In: IEEE International Conference on Robotics and Automation (ICRA), Pasadena, CA, USA, pp.1543-1548.

Alessandro Cammarata, 2012, "On the stiffness analysis and elastodynamics of parallel kinematic machines". Serial and Parallel Robot Manipulators - Kinematics, Dynamics, Control and Optimization, Dr. Serdar Kucuk (Ed.), ISBN: 978-953-51-0437-7, InTech, DOI: 10.5772/31891.

G. D. L. Soares Júnior, J. C. M. Carvalho, R. S. Gonçalves ,2011, "Stiffness analysis of 6-RSS parallel manipulator". 13th World Confress in Mechanism and Machine Science, Guanajuato, México, pp 19-25.

Charles MM, Clinton CM, Zhang G, Wavering AJ , 1997, "Stiffness modeling of a Stewart platform based milling machine". In: Transaction of NAMRI/SME, Technical Report, Institute for Systems Research. Vol. XXV, pages 335-340, Lincon.

A. Pashkevich, A. Klimchik; D. Chablat, 2009, "Nonlinear effect in stiffness modeling of robotic manipulators", In: Proceedings of International Conference on Computer and Automation Technology (ICCAT 2009), Venice, Italy, World Academy of Science, Engineering and Technology 58, pp. 168-173.

F. Majou, C. Gosselin, P. Wenger, D. Chablat, 2007, "Parametric stiffness analysis of the Orthoglide, Mechanism and Machine Theory 42, pp. 296-311.

M. Ceccarelli, G. Carbone, 2002, "A stiffness analysis for CaPaMan (Cassino Parallel Manipulator)", Mechanism and Machine Theory 37 (5), pp. 427–439.

O. Company, S. Krut, F. Pierrot, 2002, "Modelling and preliminary design issues of a 4-axis parallel machine for heavy parts handling", Journal of Multibody Dynamics 216, pp. 1–11.

R. Vertechy, V. Parenti-Castelli, 2007, "Static and stiffness analysis of a class of over-constrained parallel manipulators with legs of type US and UPS", in: Proceedings of IEEE International Conference on Robotics and Automation (ICRA), pp. 561–567.

Anatol Pashkevich, Alexander Klimchik, Damien Chablat, 2011, "Enhanced stiffness modeling of manipulators with passive joints". Mechanism and Machine Theory 46, 5 (2011) 10-18, arXiv: 1104.0769

B.S. El-Khasawneh, P.M. Ferreira, 1999, "Computation of stiffness and stiffness bounds for parallel link manipulators", International Journal of Machine Tools and Manufacture 39 (2), pp. 321–342.

R. Rizk, J.C. Fauroux, M. Mumteanu, G. Gogu, 2006, "A comparative stiffness analysis of a reconfigurable parallel machine with three or four degrees of mobility", Journal of Machine Engineering 6 (2), pp. 45–55.

K. Nagai, Zh. Liu, 2007, "A systematic approach to stiffness analysis of parallel mechanisms and its comparison with FEM", In: Proceeding of SICE Annual Conference, Kagawa University, Japan, pp.1087-1094.

X. Hu, R. Wang, F. Wu, D. Jin, X. Jia, J. Zhang, F. Cai, Sh. Zheng, 2007, "Finite element analysis of a six-component force sensor for the trans-femoral prosthesis", In: V.G. Duffy (Ed.), Digital human modeling, Springer-Verlag, Berlin Heidelberg, pp. 633–639.

C.S. Long, J.A. Snyman, A.A. Groenwold, 2003, "Optimal structural design of a planar parallel platform for machining", Applied Mathematical Modelling 27 (8), pp. 581–609.

C. Corradini, J.C. Fauroux, S. Krut, O. Company, 2004, "Evaluation of a 4 degree of freedom parallel manipulator stiffness", In: Proceedings of the 11th World Cong. in Mechanism & Machine Science (IFTOMM'2004), Tianjin, China, pp. 1857-1861.

B.C. Bouzgarrou, J.C. Fauroux, G. Gogu, Y. Heerah, 2004, "Rigidity analysis of T3R1 parallel robot with uncoupled kinematics", In: Proceedings of the35th International Symposium on Robotics, Paris, France.

G. Piras, W.L. Cleghorn, J.K. Mills, 2005, "Dynamic finite-element analysis of a planar high-speed, high-precision parallel manipulator with flexible links", Mechanism and Machine Theory 40 (7), pp. 849–862.

Wang Y.Y, Huang Tian, Zhao X., Mei Jiangping, Derekg C., 2008, “A semi-analytical approach for stiffness modeling of PKM by considering compliance of machine frame with complex geometry”. Chinese Science Bulletin, Springer, Volume 53, Issue 16, pp. 2565-2574.

Bonnemains Thomas, Chanal Helene, Bouzgarrou Chedli, Ray Pascal, 2008, “Definition of a new static model of parallel kinematic machines: highlighting of over-constraint influence”. Int. Conf. on Intelligent Robots and Systems, Acropolis Convention Center, IEEE/RSJ France.

Boyin Ding, Benjamin S. Cazzolato, Richard M. Stanley , 2013, “Stiffness analysis and control of a Stewart platform-based manipulator with decoupled sensor-actuator locations for application in biomechanical testing”. School of Mechanical Engineering, University of Adelaide, Adelaide SA 5005 Australia.

M. Mahboubkhah, M. J. Nategh, S. E. Khadem, 2008, “Vibration analysis of machine tool’s hexapod table”. International Journal of Advance Manufacturing Technologies, Volume 38, Issue 11-12, pp. 1236-1243.

M. Mahboubkhah, M. J. Nategh, S. E. Khadem, 2009, “A comprehensive study on the free vibration of machine tools’ hexapod table”. International Journal of Advance Manufacturing Technologies, Volume 40, Issue 11-12, pp 1239-1251.

Bergamaschi P R, Nogueira A C, Saramago S F., 2006, "Design and optimization of 3R manipulators using the workspace features". Appl Math Comput, 172: pp. 439-463.

Rout B K, Mittal R K., 2008, "Parametric design optimization of 2-DOF R–R planar manipulator: A design of experiment approach". Robot Cim-Int Manuf, 24: pp. 239-248.

Ceccarelli M, Lanni C. , 2004, "A multi-objective optimum design of general 3R manipulators for prescribed workspace limits". Mech Mach Theory, 39: pp. 119-132.

Mitchell J. H. Lum, Jacob Rosen, Mika N. Sinanan, et al. Optimization of a spherical mechanism for a minimally invasive surgical robot: theoretical and experimental approaches, IEEE T Bio-Med Eng, 2006, 53(7): pp. 1440 – 1445.

Chablat D, Angeles J., 2002, "On the kinetostatic optimization of revolute-coupled planar manipulators". Mech Mach Theory, 37: pp. 351-374.

Zhao J S, Zhang S L, Dong J X., 2007, "Optimizing the kinematic chains for a spatial parallel manipulator via searching the desired dexterous workspace". Robot Cim-Int Manuf, 23: pp. 38-46.

Boeij J, Lomonova E A, André J A, 2008, "Optimization of contactless planar actuator with manipulator", IEEE T Magn, 44(6): pp. 1118 -1121

Xinjun LIU, Zhidong LI, Xiang Chen., 2011, “Structural optimization of typical rigid links in a parallel kinematic machine”, Front. Mech. Eng. 6(3): 344–353, Springer Verlog Berlin, DOI: 10.1007/s11465-011-0227-x.

Holland J., 1975, "Adaptation in natural and artificial systems". The University of Michigan Press, Ann Arbor, MI.

António M. Lopes, E.J. Solteiro Pires, Manuel R. Barbosa, 2012, "Design of a parallel robotic manipulator using evolutionary computing", InTech: International Journal of Advanced Robotic Systems, DOI: 10.5772/50922.